AD-A155 035 KINETIC FRICTION COEFFICIENT OF ICE(U) COLD REGIONS 1/1
RESEARCH AND ENGINEERING LAB HANOVER NH
K A FORLAND ET AL. MAR 85 CRREL-85-6

UNCLASSIFIED F/G 8/12 NL

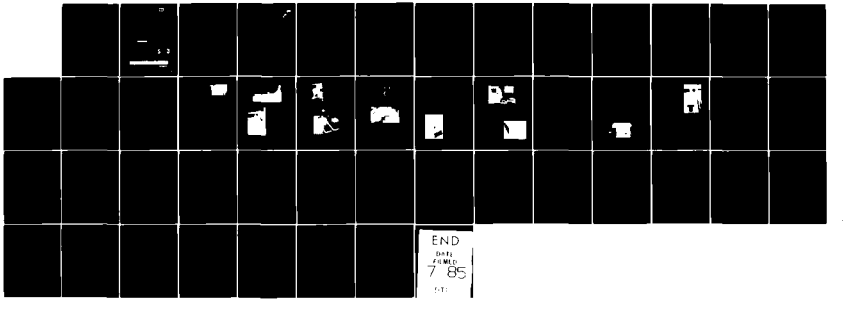

END
DATE FILMED
7-85
DTIC

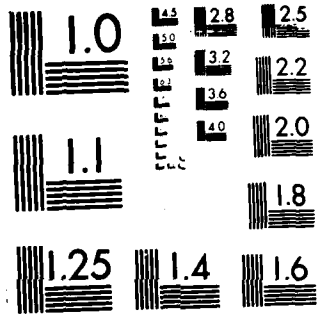

MICROCOPY RESOLUTION TEST CHART
NATIONAL BUREAU OF STANDARDS 1963-A

(2)

CRREL
REPORT 85-6

US Army Corps
of Engineers
Cold Regions Research &
Engineering Laboratory

AD-A155 035

Kinetic friction coefficient of ice

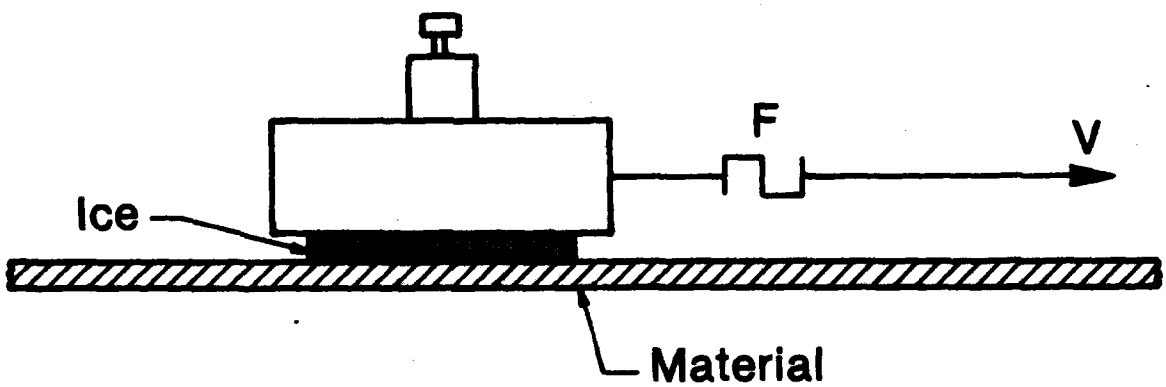

DTIC
ELECTE
JUN 17 1985
S D
G

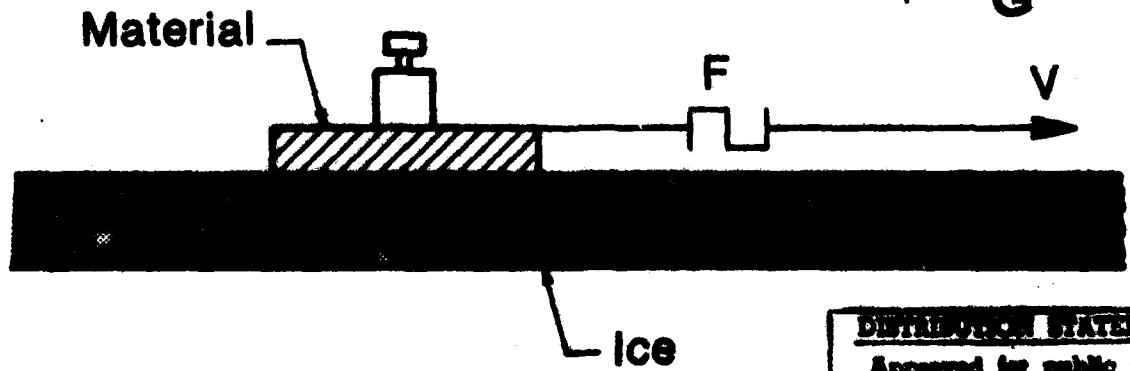

DTIC FILE COPY

DISTRIBUTION STATEMENT A
Approved for public release;
Distribution Unlimited

85 5 20 026

For conversion of SI metric units to U.S./British customary units of measurement consult ASTM Standard E380, Metric Practice Guide, *published by the American Society for Testing and Materials, 1916 Race St., Philadelphia, Pa. 19103.*

Cover: Test configurations used in friction experiments.

CRREL Report 85-6

March 1985

Kinetic friction coefficient of ice

Kathryn A. Forland and Jean-Claude P. Tatinclaux

Accession For
NTIS GRA&I
DTIC TAB
Unannounced
Justification
By
Distribution/
Availability Codes
Dist | Avail and/or Special
A/1

Approved for public release; distribution is unlimited.

Unclassified

SECURITY CLASSIFICATION OF THIS PAGE *(When Data Entered)*

REPORT DOCUMENTATION PAGE		READ INSTRUCTIONS BEFORE COMPLETING FORM
1. REPORT NUMBER CRREL Report 85-6	2. GOVT ACCESSION NO.	3. RECIPIENT'S CATALOG NUMBER
4. TITLE *(and Subtitle)* KINETIC FRICTION COEFFICIENT OF ICE		5. TYPE OF REPORT & PERIOD COVERED
		6. PERFORMING ORG. REPORT NUMBER
7. AUTHOR(s) Kathryn A. Forland and Jean-Claude P. Tatinclaux		8. CONTRACT OR GRANT NUMBER(s)
9. PERFORMING ORGANIZATION NAME AND ADDRESS U.S. Army Cold Regions Research and Engineering Laboratory Hanover, New Hampshire 03755-1290		10. PROGRAM ELEMENT, PROJECT, TASK AREA & WORK UNIT NUMBERS
11. CONTROLLING OFFICE NAME AND ADDRESS U.S. Army Cold Regions Research and Engineering Laboratory Hanover, New Hampshire 03755-1290		12. REPORT DATE March 1985
		13. NUMBER OF PAGES 45
14. MONITORING AGENCY NAME & ADDRESS*(if different from Controlling Office)*		15. SECURITY CLASS. *(of this report)* Unclassified
		15a. DECLASSIFICATION/DOWNGRADING SCHEDULE

16. DISTRIBUTION STATEMENT *(of this Report)*

Approved for public release; distribution is unlimited.

17. DISTRIBUTION STATEMENT *(of the abstract entered in Block 20, if different from Report)*

18. SUPPLEMENTARY NOTES

19. KEY WORDS *(Continue on reverse side if necessary and identify by block number)*

Friction	Kinetic friction coefficient
Ice	Model tests
Ice engineering	

20. ABSTRACT *(Continue on reverse side if necessary and identify by block number)*

This study investigates the relative influence of various parameters on the kinetic friction coefficient μ_k between ice and different surfaces. Friction tests were performed with urea-doped, columnar ice, studying the parameters of normal pressure, velocity, type of material, material roughness, ice orientation, ice hardness and test configuration. Tests were conducted by pulling a sample of ice over a sheet of material and by pulling a sample of material over an ice sheet. An ambient temperature of $-1.5 \pm 1^{\circ}C$ was maintained throughout, and the ice surface hardness was measured using a specially designed apparatus. The results of the friction tests revealed that the behavior of μ_k with varying velocity was significantly influenced by the test configuration and material roughness. The magnitude of the kinetic friction coefficient was also affected by varying normal pressure, surface roughness and ice hardness. Additional guidelines for standardized ice friction tests and future investigations were recommended.

DD FORM 1 JAN 73 1473 EDITION OF 1 NOV 65 IS OBSOLETE

Unclassified

SECURITY CLASSIFICATION OF THIS PAGE *(When Data Entered)*

PREFACE

This report was prepared by Kathryn A. Forland, graduate student, Thayer School of Engineering, Dartmouth College, and Dr. Jean-Claude P. Tatinclaux, Research Hydraulic Engineer of the Ice Engineering Research Branch, Experimental Engineering Division, U.S. Army Cold Regions Research and Engineering Laboratory.

The work described herein was made possible through funding provided by a joint program of the U.S. Army Cold Regions Research and Engineering Laboratory (CRREL) and the Thayer School of Engineering at Dartmouth College.

Dr. Devinder S. Sodhi and Dr. Virgil J. Lunardini, both of CRREL, were technical reviewers of the report. The authors express their appreciation to Dr. Francis Kennedy, Associate Professor at Thayer School of Engineering, Dartmouth College, whose suggestions enhanced the study. They also greatly appreciate the efforts of the CRREL personnel who provided both technical and administrative support to the project and especially thank C.E. Morris, A.E. Lozeau, C.L. Ackerman and the personnel of CRREL's Technical Services Division for their invaluable assistance during the study.

The contents of this report are not to be used for advertising or promotional purposes. Citation of brand names does not constitute an official endorsement or approval of the use of such commercial products.

CONTENTS

ILLUSTRATIONS

TABLES

NOMENCLATURE

a	Maximum length of elliptical contact area.
A	Contact area between ice and a material ($= nx^2$).
A_c	Circular surface area, the estimated contact region of the indentor.
A_E	Constant (Evans et al. 1976).
A_S	Surface area of the ice sample.
A_T	Real contact area between ice and a material.
b	Maximum breadth of elliptical contact area.
B	$1.74\ k_i b(a/\pi\ D)^{1/2}$.
$c_{1,2}$	Specific heat capacity, subscript 1 referring to ice and 2 to the material interacting with ice.
d	Thickness of the liquid layer produced by melting ice during sliding.
d_i	Diameter of the indentor.
dP_H	Change in hydrostatic pressure.
dT_m	Depression of the melting point because of change in hydrostatic pressure.
D	Thermal diffusivity of ice.
F	Frictional force.
F_m	Component of the frictional force arising from the heat used to melt the ice surface.
g	Acceleration of gravity.
h	Latent heat of melting for ice.
H_1	Indentation hardness of ice ($= N/A$).
H_i	Hardness index of ice determined from average penetration depth of the hardness measurement indentor.
k	Thermal conductivity of the material interacting with ice.
k_i	Thermal conductivity of ice.
n	Number of small contacts at asperities of sliding surfaces.
N	Normal load.
N_i	Normal load applied to the ice during the indentation process. During this study N_i = 17 N.
P	Normal pressure.
P_H	Hydrostatic pressure.
q	Hypotenuse of right triangle formed by indentation depth and radius of indentor contact area.
r	Radius of circular contact between ice and a material.
r_A	Radius of A_c.
R	Roughness.

S	Adhesion strength in the contact surface between ice and material.
S_A	Surface area of the indentor.
t	Time.
T	Temperature.
T_m	Melting point of ice appropriate to the applied normal pressure.
T_o	Ambient temperature.
v	Relative velocity between the sliding surfaces.
x	Side of square contact area between ice and a material.
x_i	Penetration depth of hardness measurement indentor.
Y	Yield stress of ice.
α	τ/P.
ΔS	Change in entropy because of ice-water phase change.
ΔT	Rise in temperature at the contact surface between ice and material.
$\Delta T_{1,2}$	Temperature difference between the contact surface and the bulk solid, subscript 1 referring to ice and 2 to the material interacting with ice.
ΔV	Change in volume because of ice-water phase change.
η_0	Viscosity of water, sea water or brine.
μ_k	Coefficient of kinetic friction.
μ_m	F_m/N.
$\varrho_{0,1,2}$	Density, subscript 0 referring to water, 1 to ice and 2 to the material interacting with ice.
σ_f	Flexural strength.
τ	Frictional shear stress.
τ_0	Effect of adhesion on the frictional shear stress of ice.

KINETIC FRICTION COEFFICIENT OF ICE

Kathryn A. Forland and Jean-Claude P. Tatinclaux

INTRODUCTION

Before making a large financial investment in building a structure designed for use in an ice environment, it is wise first to model its performance to ensure its success. The structure, for example, may be an icebreaking vessel, an artificial island for arctic oil procurement, or a bridge across an ice-prone river. Before modeling a structure, the significant parameters affecting its performance must be identified, and in order to obtain repeatable and comparable results, standardized procedures should be followed in quantifying these parameters.

In an effort to control better the procedures for testing ice properties, the International Association of Hydraulic Research (IAHR) established a working group whose charter was to formulate standard procedures or guidelines for testing the mechanical properties of ice. The committee's first recommendations (Frankenstein 1975) outlined methods of testing ice in uniaxial tension and compression. Subsequent publications (Schwarz 1979, Michel et al. 1981) discussed the working group's guidelines for flexural strength measurements from in situ cantilever beams, strain measurements in ice, multiaxial testing and friction measurements. These guidelines are intended for improving the "quality, comparability and usefulness" of data on ice properties (Frankenstein 1975). The committee expects that the testing procedures will be improved, corrected and expounded upon as new information is gathered.

Among the ice properties that significantly affect ice forces on structures, the friction coefficient between ice and the structure's surface is certainly the most difficult to quantify. In addition to the IAHR working group's procedures for ice friction measurements (Appendix A), specific conditions were set by the Committee on Ships in Ice-Covered Waters (1981) during the 16*th* International Towing Tank Conference (ITTC) for model tests of an icebreaker. These requirements (Appendix A) were established in an effort to ensure consistency in the methods for measuring the coefficient of friction. However, before different investigators can use a standardized friction factor test for comparing results, it is necessary first to identify and then to gain a greater understanding of those parameters that significantly affect ice friction.

A review of recent work in the area of ice friction reveals much disagreement among the results of different investigations. All studies accounted for normal pressure, velocity, temperature, and material interacting with the ice, but little attention was given to the variability of ice characteristics, such as hardness or strength, or to variations in the testing setup, which are also likely to have a significant effect on the ice friction factor. This study attempts to clarify some of the discrepancies and to identify more completely the parameters that affect the kinetic friction of ice.

LITERATURE REVIEW

Friction tests

The kinetic friction coefficient or friction factor μ between any two surfaces moving relative to one

another is defined as $\mu_k = F/N$ where F is the frictional force and N is the normal load. Historically, most investigations of ice friction have attempted to quantify the friction coefficient between freshwater ice and a skate or ski. However, many recent studies of ice friction have been conducted by researchers in ice engineering who are interested in friction forces on a structure in an ice environment. A chronological discussion of a number of these studies follows.

Bowden and Hughes (1939) theorized that water, resulting from the frictional heating of ice, would act as a lubricant during sliding and lower the friction factor. Their basic testing configuration was that of a sample moving relative to a larger body of ice.

They concluded that water from the melting ice did reduce the friction factor. They also found that varying the sample size had no effect on the coefficient of friction, and that it was nearly independent of the normal load, providing that the load was not "too great." Over a certain range velocity had no effect, but higher friction factors resulted when the velocity was "low." (Table 1 summarizes Bowden and Hughes' [1939] study, along with those that follow.)

Barnes et al. (1971) studied ice friction in conjunction with tests to determine the creep behavior of polycrystalline ice. The friction tests were conducted under conditions of strong interfacial adhesion by sliding the tip of a conical piece of ice over a test surface.

They found that the frictional force was nearly proportional to the normal pressure and nominal area. Tests studying the effects of varying velocity on the friction factor between ice and granite resulted in data that, when plotted as friction factor versus sliding speed, took the form of a bell-shaped curve, convex upwards. They also concluded that the rise in temperature at the contact surface ΔT varied according to the equation

$$\Delta T = \frac{\mu N g v}{4r} \frac{1}{k_i + k} \qquad (1)$$

where r = radius of the circular contract area
v = velocity between the sliding surfaces
k_i = thermal conductivity of ice
k = thermal conductivity of the material interacting with ice
g = acceleration of gravity.

An insulating material such as granite resulted in a large rise in the temperature of the contact surface during sliding. This frictional heating melted the surface of the ice, and the lubricating properties of the meltwater caused a drop in the friction coefficient. Tests were also conducted with steel with a surface asperity roughness of about 0.5 μm; there was no variation in the friction coefficient with a velocity increase from 10^{-6} to 10^{-1} m/s.

Enkvist (1972) investigated ice friction in relation to the ice resistance encountered by icebreaking ships. His tests were performed both in the field by towing sleds across natural ice of 0.9 ‰ salinity and in the laboratory by pulling metal plates across ice and model ice across the test surfaces.

These field and laboratory tests revealed that the coefficient of friction is practically independent of velocity within the range of 0.25 to 1.75 m/s, indicating that viscous forces are unimportant. The friction factor decreased with increasing normal pressure, becoming nearly constant in the field tests with pressures above approximately 16 kPa. In the laboratory tests, the kinetic friction factor appeared to depend on the type of surface roughness rather than the degree of roughness. The friction coefficient also decreased with increasing normal load until a pressure of approximately 1.3 kPa, beyond which the friction factor became constant. Enkvist concluded that the surface of models used for icebreaking model tests may have the greatest influence on the results.

Also looking at icebreaker resistance, Ryvlin (1973) performed field experiments by towing steel specimens over freshwater ice and sea ice. The specimens were cylindrical steel sheets.

In all cases, both with freshwater ice and with sea ice, no significant change in μ_k with increasing velocity was observed. It was independent of normal pressure when normal pressure was greater than 10 kPa, but it increased with decreasing pressure below 10 kPa. The variation of ambient temperature as well as the roughness of the ice surface had no significant effect on μ_k. Laboratory tests that were conducted by towing saltwater ice samples over steel and wood showed that μ_k was far greater for rusty steel than for either polished steel or painted wood.

The study of ice friction conducted by Evans et al. (1976) expounded upon the idea, first supported by the work of Bowden and Hughes (1939), of sliding surface lubrication by meltwater from frictional heating. They concluded that it was possible to calculate the dependence of the friction factor on the thermal conductivity of the material interacting with ice, the relative velocity between ice

and the material, and ambient temperature. In their pendulum-type apparatus, sliders of the material being tested were supported above a drum of ice rotating about its horizontal axis. The ice was made from ordinary tap water. Their results show that at -11.5°C, the coefficients of friction between ice and sliders of copper, Perspex and mild steel increased nearly linearly with $v^{-1/4}$, where v, the velocity, varied between 0.2 and 10 m/s.

Evans et al. (1976) theorized that the friction factor between ice and a material is determined by the heat flow at the contact surface rather than the energy expended in shearing the interface. They thought that the heat from the contact surface was dissipated partly by means of the latent heat of the meltwater produced during sliding but mainly through conduction into the sliders and the ice. Because the temperature of the contact surface was assumed to be constant at the melting temperature, the effects on the friction factor of variables such as velocity or ambient temperature could be calculated by knowing the thermal conductivity of the material interacting with ice. They developed an equation that can be used to determine the friction coefficient as long as the contact area and thermal constants of ice are known:

$$\mu = \frac{A_E k(T_m - T_0)}{N v} + \frac{B(T_m - T_0)}{N v^{1/4}} + \mu_m \quad (2)$$

where $B = 1.74 k_i b(a/\pi D)^{1/4}$ and $\mu_m = F_m/N$. The constant A_E depends on the size of the contact area, the geometry of the slider and the nature of its surface. The area of contact is assumed to be elliptical with a being the maximum length and b the maximum breadth. The thermal diffusivity of ice is D, and F_m is the component of the frictional force arising from the heat used to melt the ice surface. The ambient temperature is represented by T_0, and T_m the melting point of ice appropriate to the pressure.

During an investigation of ice forces, Saeki et al. (1979) studied the coefficient of friction between sea ice from the Okhotsk Sea, Japan, and various materials used in offshore structures by moving a cylindrical ice sample over test surfaces. The test surfaces were concrete plates and various steel plates, which were uncoated, rusty or coated with marine paint.

There appeared to be to be no effect on μ_k from varying normal pressure. There also was no variation in μ_k with velocities ranging from 0.7 to 8 cm/s. However, the type of material interacting with the sea ice significantly influenced the value of the friction factor.

Vance (1980) conducted field tests for ice friction by pulling a loaded freshwater ice block across uncoated steel or steel coated with Inerta 160. The test results showed an increase in μ_k with increasing velocity and a decrease in μ_k with increasing load or normal pressure.

Tusima and Tabata (1979) and Tabata and Tusima (1981) conducted ice friction tests in the laboratory using samples of sea ice. They felt (Tusima and Tabata 1979) that a rough estimate of μ_k for ice could be obtained using the equation

$$\mu_k = S/Y \quad (3)$$

where S is the adhesion strength in the contact surface between ice and a material and Y is the yield stress of ice. They assumed that μ_k was independent of the apparent contact area and the normal load.

Their test results indicated that μ_k was independent of the normal pressure, and that μ_k decreased with increasing velocity. Tusima and Tabata (1979) assumed that if liquid brine or seawater act as a lubricant, the frictional force should vary with velocity as

$$F = \eta_0(v/d)A_T \quad (4)$$

where η_0 is the viscosity of the liquid, d is the thickness of the liquid layer and A_T is the real contact area.

Tests conducted by Tabata and Tusima (1981) with stainless steel plates of varying roughnesses resulted in a linear increase in kinetic friction with increasing root mean square roughness. This trend suggests the importance of a ploughing effect on the coefficient of kinetic friction between ice and a rough surface.

Calabrese and Buxton (1980) and later Calabrese and Murray (1982) used the same apparatus in their laboratory tests of ice friction. Their tests investigating the effect of increasing material roughness on the kinetic friction factor revealed only a slight increase in μ_k with increasing roughness. The effect of varying velocity on the friction factor between ice and 1018 steel was evaluated by continuously measuring the frictional torque. The friction factor gradually decreased from the static value as the velocity increased. They also found no apparent effect of normal load on the ice friction coefficient.

Oksanen (1980, 1983) theorized that when ice moves relative to a material, the frictional heat that results from sliding is dissipated by conduction into the bulk solids and by the latent heat of

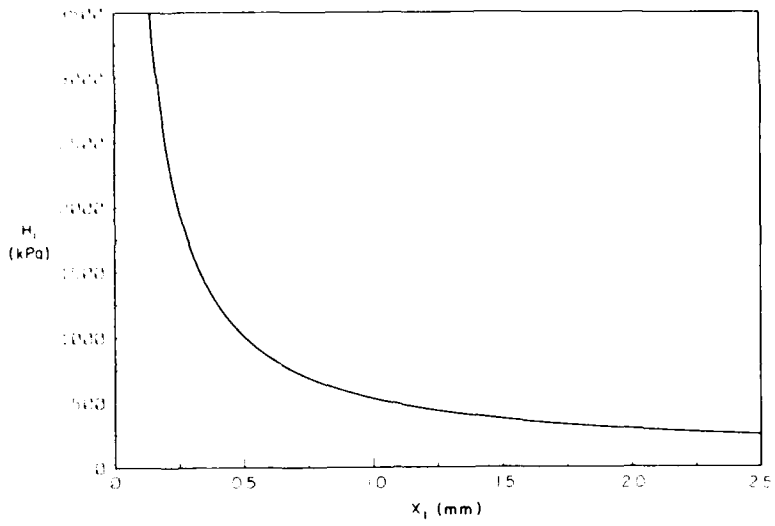

Figure 14. Hardness value H_i *versus the hardness index* x, *according to eq 10.*

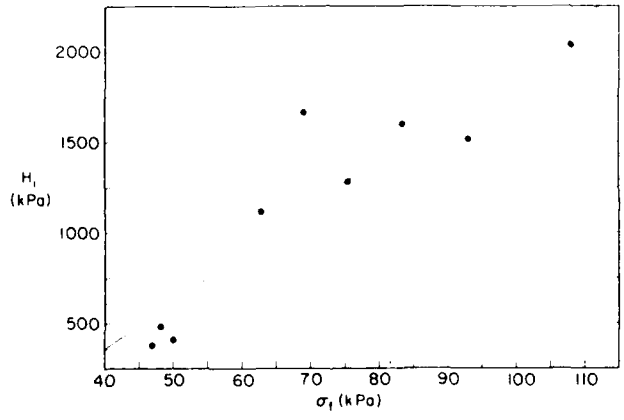

Figure 15. The hardness value H_i *versus the flexural strength* σ_f *of a CRREL test basin ice sheet.*

grown in the CRREL test basin, were achieved by tempering the sheet at an ambient air temperature of 1 °C. The hardness index varies linearly with the flexural strength of ice. The slope of 26.3 and the correlation coefficient of 0.92 were calculated from linear regression analysis of the data.

Because tests were conducted at ambient air temperatures of -1.5 ±1 °C during this study, it is possible, according to Barnes and Tabor (1966), that pressure melting may contribute to the indentation hardness measurements that were made at ice temperatures above -1.2 ±0.3 °C. Since the ice temperature was allowed several hours to reach steady state prior to testing, it is assusmed that the ambient and ice temperatures were very close to each other during the testing (Appendix C). According to eq 7 a hydrostatic pressure of 6.8 MPa is required to cause pressure melting at the highest testing temperature of -0.5 °C. The hardest ice used during this investigation had an average indentor penetration depth of 0.15 mm, which corresponds to a hardness value of 3.3 MPa. The hydrostatic stress that causes pressure melting is 60% of the hardness value (Barnes and Tabor 1966), indicating that pressure melting should not contribute to indentations of 0.15 mm that resulted from hydrostatic pressures of 2.0 MPa.

It should again be emphasized that the hardness index of this investigation is intended for comparison only within this study. The application of the

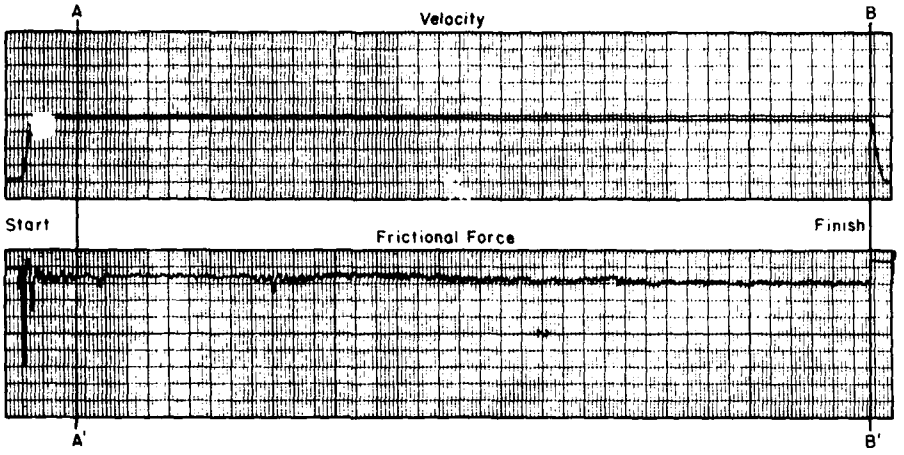

Figure 12. Records of velocity and frictional force versus time for a typical test performed by pulling a sample of stainless steel (0.36 μm RA) over the top surface of an ice sheet (P = 10 kPa, v = 10 cm/s).

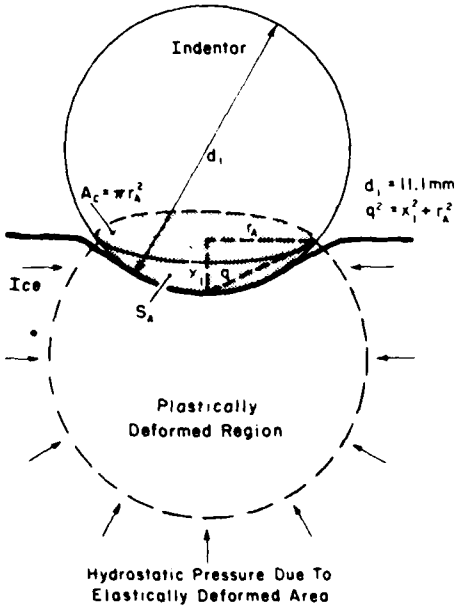

Figure 13. The contact area between the hardness indentor and the ice surface was approximated as circular. The penetration depth x_i was measured directly by the hardness indicator.

$A_c = \pi r_A^2$, according to Figure 13. The shaded surface area S_A of the indentor of diameter d_i is determined by (Selby 1973)

$$S_A = \pi d_i x_i = \pi q^2 \tag{8}$$

in which $q^2 = x_i^2 + r_A^2$. The hardness of the ice H_i is defined as N_i/A_c, where N_i is the normal load applied to the ice during the identation process. Therefore, the hardness H_i varies with the average penetration depth x_i according to the expression

$$H_i = \frac{N_i}{\pi(d_i x_i - x_i^2)} \tag{9}$$

In this study, 17 N was used as the normal load applied to the hardness apparatus. In addition, the small ball bearing with d_i = 11.1 mm was used. Equation 9 can then be reduced to

$$H_i = \frac{48.9}{(x_i - 0.90x_i^2)} \text{ kPa} \tag{10}$$

where H_i is expressed in kPa and the penetration depth x_i is given in centimetres. Figure 14 shows the hardness index given by eq 10 versus the average penetration depth of the indentor. The standard deviations of the hardness measurements varied from 9 to 21% for ice used in the sample room tests. The harder ice of the test basin experiments had relatively large standard deviations, 43% in one case, because of the small indentation depth of hard ice as well as the accuracy of the dial indicator and method of reading the dial.

Further significance of the hardness index for top ice is given in Figure 15 where the hardness is plotted versus flexural strength σ_f. The flexural strength of the ice was determined from in situ cantilever beam tests by the method discussed by Timco (1981). The different flexural strengths and corresponding hardnesses of a single ice sheet,

uration c (Fig. 1c) by pulling the steel sheet beneath a fixed, loaded sample of top ice that had been cut from the same ice sheet.

During tests on the effects of varying roughnesses on the kinetic friction coefficient between ice and the stainless steel sheet, the ice samples were pulled in both directions over the material surface to eliminate any effects attributable to the possible bias of the roughnesses.

Test basin experiments

The procedure for tests performed in the CRREL test basin varied only slightly from the standard procedure discussed in the previous section. The load cell and data acquisition system were checked and the initial hardness test was made. After the specimen was positioned at the start position, the normal load was carefully applied to the top of the sample. At the end of the run the load was removed from the specimen, the sliding surface of the sample was wiped dry, and the sample was then placed at the start position for the next run. Two runs were typically made for each set of experimental conditions. The motor-pulley assembly was then moved to an adjacent track of ice that was free of any rough spots, and the next series of tests were done.

Friction experiments were also conducted so that the effects on the friction factor of test configurations a and b (Fig. 1) could be directly compared using the same test environment and ice from the same sheet. The stainless steel sheet from the sample room experients was placed on the test basin ice sheet, an ice sample was cut from the test basin ice, and the friction tests on the sheet of material were conducted in the same manner as the sample room experiments (Fig. 11).

Figure 11. Friction experiments conducted with a top ice sample on the stainless steel sheet in the CRREL test basin.

RESULTS

Figure 12 shows the records of velocity and frictional force versus time for a typical test of a sample of stainless steel (0.33 μm RA) being pulled over the top surface of an ice sheet. The relative velocity was approximately 10 cm/s and normal pressure was 10 kPa.

In this example, as in all the tests, the kinetic friction factor was calculated from the average frictional force that resulted after the velocity had reached a constant value, that is, over the period between AA′ and BB′ on Figure 12. The coefficient of kinetic friction was then calculated as the ratio of this average frictional force to the combined normal force of applied load and sample weight.

One of the main findings of this study is that results of ice friction tests are strongly affected by the test configuration and testing method, specifically whether sliding occurs between a loaded ice sample and a sheet of material (Fig. 1a) or between a loaded sample of material and an ice sheet (Fig. 1b). For this reason, the test results pertaining to these two types of testing methods are presented in separate sections below. The significant data of this investigation are listed in Appendix B, which is divided into tables according to the parameters investigated.

Hardness index

The actual hardness index of ice can be determined from the average penetration depth of the hardness indentor x, by approximating the contact region of the indentor as a circular surface area,

ed by the skill of the operator. No instrumentation was used during loading, but to maintain repeatability in the tests, the first author performed all hardness measurements.

Each hardness test consisted of three or more indentation trials performed near the center of the ice specimen using either of the ball bearings. Indentation readings for the ice top surface were taken using both the small and large ball bearings. The ice sample was then flipped, and indentation readings for the ice bottom surface were taken using only the large ball bearing. The hardness index of an ice sample was simply determined from the average of these displacements or indentations. Initially, hardness measurements were only made once during an experiment. Later in the testing schedule, hardness measurements were made at the end of the testing procedure as well as at the beginning. In addition, if the testing period extended more than 2 hours, hardness tests were performed throughout the experiment.

Sample room friction tests

Prior to each series of tests, the calibration constant of the load cell was checked, and the data acquisition system was run through a dummy test to ensure that all was operating correctly. After measuring the hardness of the ice surface, an over-sized ice sample was cut from the sheet, and trimmed to the desired testing size.

The first sample to be cut for any sequence of experiments was weighed, with the sample holder, in order to determine the extra weight needed to achieve the desired normal pressure. The specimen was placed in the sample holder with the correct number of plywood shims so that about 3-6 mm of ice extended beyond the box (Fig. 10). The sample holder and ice were then placed directly on a triple-beam balance scale, and the weight was recorded.

Before the ice sample was placed at the starting point of the experimental run, the load cell was connected to the sample holder, and the sliding surface of the test material was wiped clean of any ice. The normal load was then slowly and carefully applied to the top of the sample holder. While holding the load cell cable so that it would not drag, the operator switched on the motor that pulled the ice sample along the sliding surface. At the end of the run, the normal load was removed from the sample holder, the ice specimen was moved back to the start position, the sliding surface was wiped to remove any water and ice chips left from the previous run, and the run was repeated. Typically, three runs under nominally identical test conditions were made with one ice sample. A new ice sample was cut for the next set of conditions to be tested following the same general procedure.

Relative motion effects on the kinetic friction coefficient were determined by first measuring μ_k that resulted from pulling a loaded sample of top ice over a fixed stainless steel sheet (Fig. 1a). The friction coefficient was then measured for config-

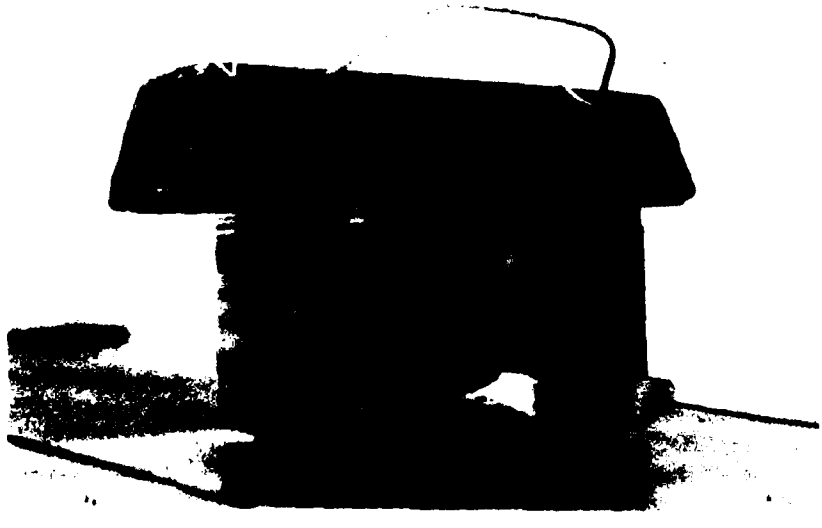

Figure 10. The loaded sample holder with 3-6 mm of ice extending beyond the box. The load cell is connected directly to the sample holder.

insulation of the sides and bottom of the tank was necessary as was the use of heat tapes to maintain a temperature slightly above 0°C at the tank bottom. During the ice growth process, the container was totally surrounded by an atmosphere well below freezing, and if these precautions were not taken, large dendritic ice crystals would grow on the tank bottom and sides, break loose, float upward and become imbedded in the ice growing at the ice/water interface. In addition, a hose, wrapped in heat tape to stop freezing, was attached to the tank drain and its open end was made level with the water surface in the tank to provide pressure relief during ice growth.

EXPERIMENTAL PROCEDURE

Ice growth

The growth of ice sheets in the CRREL test basin has been described in detail by Hirayama (1983). The procedure for growing ice sheets in the tub was adapted from that used in the test basin. The mechanical properties and thickness of an ice sheet will be uniform if the temperature of the water before ice growth and the crystal size of the ice sheet are uniform. The urea water in both the test basin and the tub was cooled by heat exchange at the air/water interface. To ensure uniform water temperature, the water in the test basin is circulated longitudinally by pump and vertically by air bubblers; the water in the tub was simply stirred manually. The water was cooled continually until it reached approximately -0.1°C. The water surface was then skimmed to remove any needle crystals that might have formed, and the ice sheet was initiated by wet seeding. The seeding procedure involved spraying a fine mist of urea water into the air above the tank or tub where ice crystals formed; these then settled on the water surface, creating an ice skim. The crystal *c*-axis orientation of this initial skim is random. As ice growth continues, however, crystals with horizontal *c*-axis grow preferentially, resulting in a columnar ice sheet.

The seeding procedure was conducted in the test basin at a temperature of -10°C (14°F) to avoid freezeup of the spray nozzle; the growth temperature of the test basin ice sheet was -18°C (0°F). In the sample room, the ice sheet was seeded at the same temperature as the growth temperature, which varied from -18°C (0°F) to -10°C (14°F), depending upon the refrigeration needs of other coldrooms.

Once the tub or test basin ice sheet had grown to a suitable thickness, the ambient temperature was raised to -1.5 ±1°C. Five or more hours were then allowed for the ice to reach thermal equilibrium before the actual tests would begin (see Appendix C). The sample room investigations required an ice thickness of 3–4 cm, but a thick ice sheet of 6–7 cm was necessary for the test basin experiments so that deflection during the tests was minimized. In order to investigate the effects of various hardnesses on the friction coefficient, it was sometimes necessary to temper the ice sheet in the test basin by raising the ambient temperature to 1°C for several hours before reaching equilibrium at the testing temperature of -1.5°C. The hardness of the sample room ice sheet would gradually decrease over a period of several hours without requiring a change in ambient temperature from -1.5°C.

Hardness test

Hardness tests, at an ambient air temperature of -1.5 ±1°C, were done in the same manner for both the sample room and test basin experiments. As a precaution, they were done on ice samples cut from the ice sheet, rather than directly on it, to avoid the risk of a ball bearing dropping to the tub or tank bottom had it broken through the ice.

An ice specimen, cut to no particular size, was placed in the sample box, and the hardness indicator was positioned above the sample. The ball bearing was first dropped on the ice surface near a corner of the specimen, and the rod was positioned on the ball bearing. The hardness instrument was then rolled into a position near the center of the ice sample, and the dial indicator was zeroed. A 1.8-kg (4-lb) brass weight was eased into place by the operator, a process that consistently required 3 seconds. Once the 1.8-kg (4-lb) load was in place, the dial indicator reading was immediately recorded. Creep occurred readily under these conditions, and it was necessary for the operator to judge the immediate effect of applying the load to the indentor by watching the needle on the dial indicator. The needle advanced as the load was applied, and then slowed down but continued to move as creep continued. Consequently, the indentation readings were only accurate to three units on the dial (±0.075 mm).

A 1.8-kg (4-lb) weight was the standard load used in this test because its use resulted in a significant indentation without crushing the ice surface, except when the ice was extremely soft. Control over the rate at which the weight was applied was limit-

Figure 8. Data acquisition equipment used during sample room tests.

channel once every 7 ms and storing a total of 10080 data points. Since two channels were required to measure both velocity and pulling force, 5040 scans per channel were possible. The data were stored in digital form on tape cartridge by the HP9835B and on disk by the HP9845B for subsequent analysis. In order to ensure that all equipment was in working order, signals from both the load cell and magnetic pickup were monitored on a Gould Brush 260 strip chart recorder during the test basin experiments and during the sample room tests on a HP7100B and later a Gould Brush 222 strip chart recorder, the latter having a faster response.

Ice growing container

The ice used in the sample room tests was grown in a specially built tank (Fig. 9) with inside dimensions of 2.4 by 0.6 by 0.3 m (8 by 2 by 1 ft). In order to achieve in the small tank columnar ice similar in structure to that grown in the test basin,

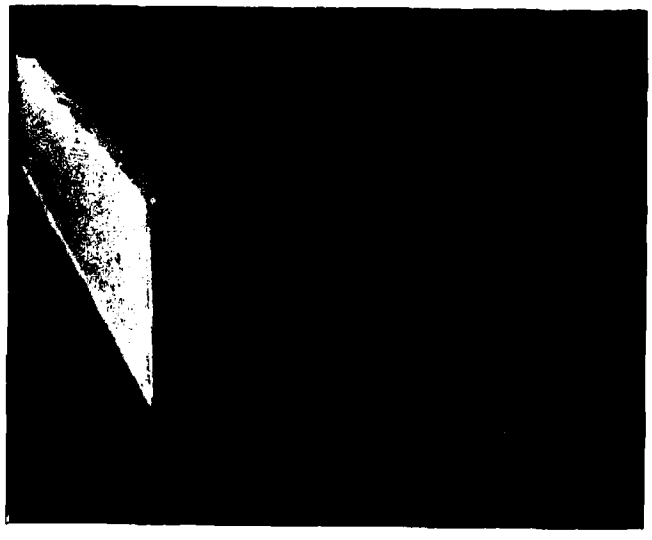

Figure 9. Container for growing ice used in sample room tests.

Table 2. Surface roughness (μm RA) of stainless steel and aluminum samples used in test basin experiments.

			Sanded			
	As-delivered	*Polished*	*36-grit*	*100-grit*	*Sandblasted*	*Sand-abraded*
Stainless steel	0.33	0.25	1.50	—	3.42	—
Aluminum	0.30	0.07	3.03	1.34	5.86	9.83

screwed directly to either the ice sample holder or the material sample and attached to the pulling cable. Depending on need, a load cell with a rated capacity of 44 N (10 lb), 222 N (50 lb) or 445 N (100 lb) was used. The drag cable was wrapped around a 70-mm (2.75-in.) pulley mounted on the output shaft of the motor. The motor rpm and resulting pulling velocity were measured by a magnetic pickup device mounted close to a wide-toothed gear that was driven indirectly by the motor shaft. The rpm of the shaft was geared up for better resolution of the magnetic pickup measurement.

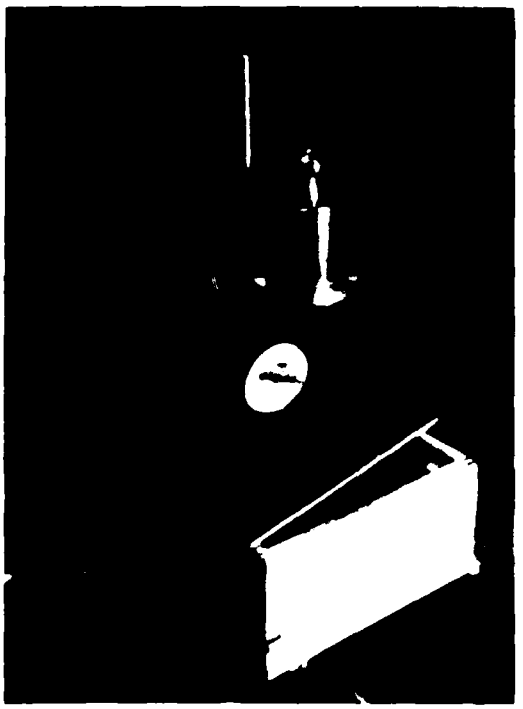

Figure 7. Hardness measurement apparatus.

Hardness measurement apparatus

As mentioned in the *Introduction*, the hardness of the ice surface was thought to have an important effect on the friction coefficient of ice. Information on the relative hardness of the ice surface was obtained during this study by a specially designed hardness indicator (Fig. 7). The main components of this hardness instrument were a Starrett dial indicator, two sizes of ball bearings or indentors with diameters of 11.1 mm (7/16 in.) and 12.7 mm (1/2 in.), an indentor rod and a weight platform. The 20- by 20- by 10-cm sample box was inverted and used as part of the apparatus to house the ice sample being tested and to support the hardness instrument on a board above the ice specimen. The level of the ice surface was adjusted by means of plywood shims so that it was nearly even with but always below the top edge of the inverted sample holder. A hole cut in the board supporting the hardness indicator allowed the ball bearing to rest on the ice surface, and the indentor rod was supported by the ball bearing. Scribed circles on the weight platform allowed brass weights up to 4.5 kg (10 lb) to be easily centered during the indentation test.

Data acquisition equipment

The basic layout of the data acquisition system used during this investigation is shown schematically in Figure 8a. The output signal of the magnetic pickup device first passed through a frequency-to-voltage converter before being sent to the Neff system-620 series-100 amplifier/multiplexer and series-300 signal conditioner, which also scanned the output signal of the load cell. The low-pass filter of the Neff system was set at 1 Hz for the velocity signal and 10 Hz for the load cell signal, and the respective amplifications were 10 and 200. The Neff system was controlled by a HP9835B desk-top computer during the sample room tests (Fig. 8b) and a HP9845B desk-top computer during the test basin experiments. Both computers were programmed with the capability of sampling each

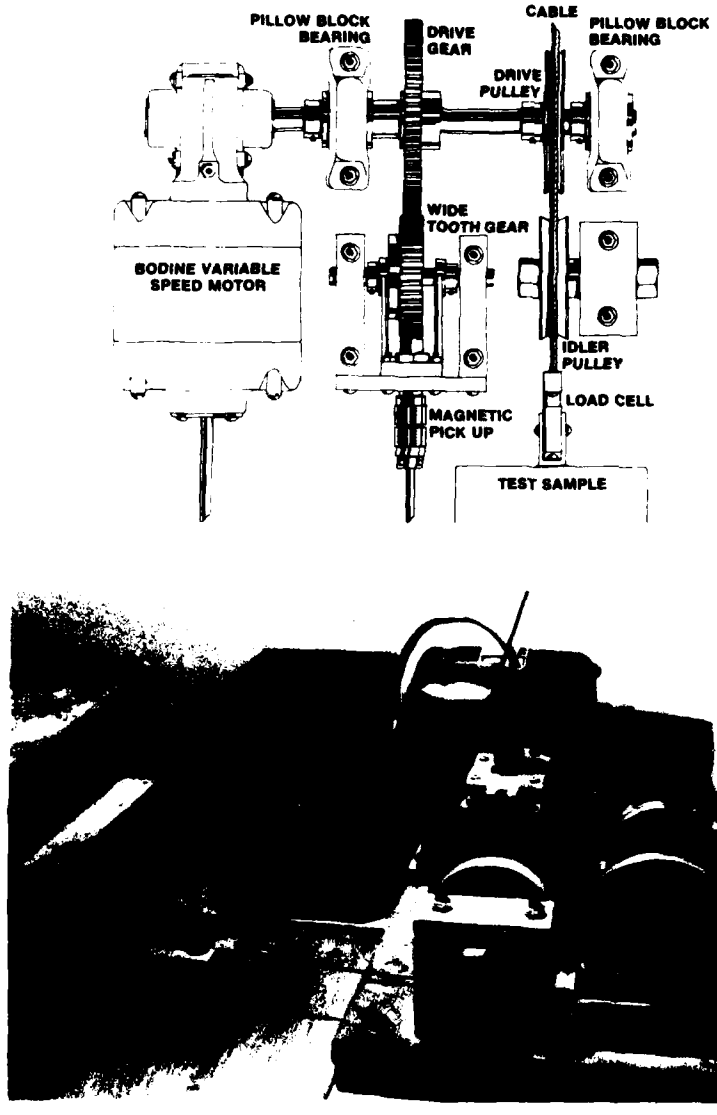

Figure 6. Basic towing apparatus with frictional force and velocity measurement devices.

nesses (Fig. 4); the as-delivered surface (0.36 μm RA), a surface sanded with 36 grit sandpaper (1.11 μm RA), and sandblasted surfaces (7.03 μm and 7.07 μm RA).

The material samples used during the test basin experiments (Fig. 5) had curved leading edges to prevent gouging of the ice sheet, and each had a sliding surface area of 14 by 14 cm. The roughnesses of the four stainless steel samples, and of the four aluminum samples (1.27 mm thick) are shown in Table 2. The Inerta 160 material, RA of 1.61 μm, received no surface treatment beyond the manufacturer's coating process, and only one sample was tested.

Basic towing apparatus

The main experimental apparatus (Fig. 6) consisted of a pulling mechanism and of force and velocity measurement systems. The pulling mechanism was driven by a 93-W (1/8-hp) Bodine variable speed motor with a torque rating of 6.1 N-m (54 lb-in.). The motor speed was geared down internally with a ratio of 20:1 to a maximum of 86 rpm. The pulling force was measured by a load cell

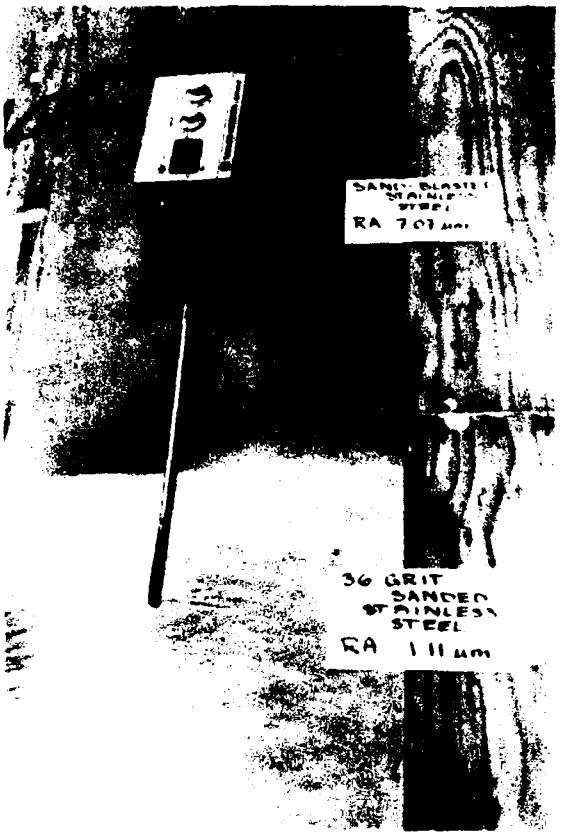

Figure 4. Stainless steel sheet and roughness measurement apparatus used during roughness study in the sample room. One side of the steel sheet was divided into areas of sandblasted surface and surface sanded with 36-grit sandpaper. A Taylor-Hobson Surtronic 3 Profilometer was used to measure roughness average.

Figure 5. Stainless steel, aluminum and Inerta 160 samples used during the test basin experiments. The surface roughnesses decrease from the front sample to the rear.

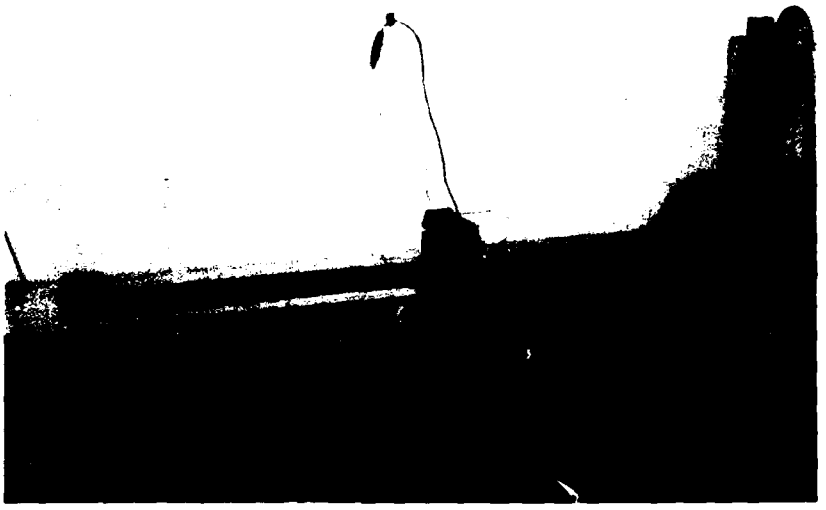

a. Sample room apparatus.

b. Test basin apparatus.

Figure 3. Experimental setup for ice friction tests.

3a) made it possible for the ice specimens to travel 2 m, excluding the required startup and stopping space. The converse configuration of towing the sample material over an ice sheet was conducted in the large test basin (34.4 by 9 m), where the travel distance was approximately 4 m (Fig. 3b).

Ice and material test samples

During the sample room experiments, a sample holder was used to pull the ice specimen along the sheet of material. Four plywood boxes with inside dimensions of 20 by 20 by 10 cm, 14 by 14 by 10 cm, 8 by 8 by 10 cm and 4 by 4 by 10 cm were used. The 14- by 14- by 10-cm box was later chosen as the standard sample holder because an ice sample with a surface area of 14 by 14 cm was large enough to be easily handled, and a sufficient number of such samples could be cut from the limited ice supply. The 4 by 4-cm samples were very difficult to handle and were soon eliminated from the testing program.

A 304-stainless steel sheet with dimensions of 2.75 by 0.3 m by 1.91 mm (9 by 1 ft by 0.075 in.) was the primary material tested during the sample room experiments. The as-delivered surface of the sheet was used while parameters other than roughness and material were investigated; its roughness average (RA) of 0.36 μm was measured with a Taylor-Hobson Surtronic 3 profilometer. In order to investigate the effects of various roughnesses on the friction coefficient, the surface of the sheet was later divided into sections of different rough-

5. Characteristics of the ice:
   a. Type.
   b. Hardness.
   c. Orientation (top or bottom).
6. Material surface interacting with ice:
   a. Type of material.
   b. Roughness of surface.

A thorough investigation of each of these parameters would require much more time and resources than were available. Therefore, the main variables selected were normal pressure, velocity, roughness and test configuration, whereas ice hardness, ice orientation and type of material were limited in variation. The ambient temperature and ice type were held constant.

In keeping with the standard ambient temperature of -0.5°C set by the 16*th* ITTC (Appendix A), a temperature of -1.5 ±1°C was used throughout this study. Because of the limitations of the coldrooms used during the investigation, it was necessary to allow for temperature fluctuations without exceeding the standard. The ice type was restricted to the urea-doped, columnar ice (Fig. 2) available at CRREL's Ice Engineering Facility. Urea ice was developed as a model ice, in order to simulate sea ice applications with a urea ($NH_2 \cdot CO \cdot NH_2$) concentration of 1% by weight in solution with fresh water (Timco 1979, 1981; Hirayama 1983).

The scope of this investigation required some measurement of ice hardness so that relative comparisons could be made between results from different friction experiments within this study. A repeatable procedure for quantifying ice hardness was developed and is outlined later in the text. The ice orientation, i.e., sliding surface, was varied between the ice top (ice/air interface) and the ice bottom (ice/water interface), with the majority of the tests conducted using the ice top. Three materials were tested with ice: bare stainless steel, bare aluminum and steel coated with Inerta 160.

During the tests on normal pressure effects, the pressure on the test specimens was varied over the range of 1–40 kPa by either changing the sample size or the normal load, or both. The upper pressure limit was chosen to be consistent with the standards set by the 16*th* ITTC, assuming a minimum scaling factor of 10. In these tests a velocity of 10 cm/s was used.

The effect of velocity on the kinetic friction coefficient was investigated by using velocities ranging from 5–25 cm/s while keeping the normal pressure at 10 kPa. During tests investigating the effects on μ_k of the parameters other than velocity and normal pressure, a velocity of 10 cm/s was used and the normal pressure was held constant at 10 kPa.

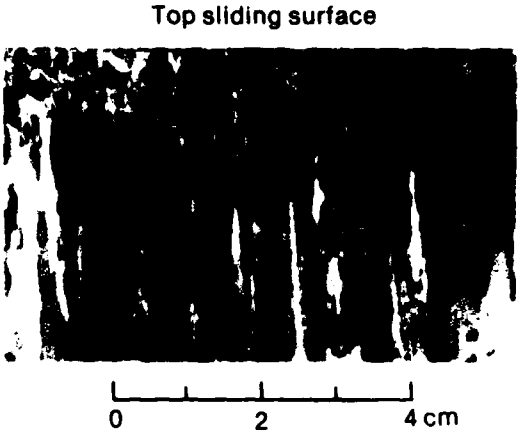

Figure 2. Thin section of urea-doped column ice.

The variation of the kinetic friction coefficient with surface roughness was studied for both stainless steel and aluminum, but since aluminum is the softer of the two materials, it was possible to investigate a wider range of roughnesses of the aluminum samples. The combined effects of varying velocity and surface roughness were also studied.

In order to determine the influence of the testing technique on the kinetic friction factor, various test configurations (Fig. 1) were investigated, in particular, when the moving ice sample continuously encounters new material (Fig. 1a) or the moving sample of material continuously encounters new ice (Fig. 1b). The fundamental difference between a loaded sample of ice moving (Fig. 1a) or held stationary (Fig. 1c) on a sheet of material was also briefly investigated. Because of the impracticality of the experimental setup, the last test configuration (Fig. 1d) was ignored.

EXPERIMENTAL APPARATUS

The experiments were done in controlled temperature areas of CRREL's Ice Engineering Facility. Friction coefficients between ice and materials were investigated in a small refrigerated room (5 by 3 m), known as the sample room, where ice samples of various sizes were towed along sheets of different materials. The 0.6- by 3-m (2- by 10-ft) testing table used in the sample room (Fig.

Surface hardness of ice

The frictional behavior of a material is affected by surface hardness because of the influence of hardness on surface deformation during sliding. The hardness of any solid is defined as the ratio of the applied normal load to the projected area of the indentation. A surface indents when a normal load is applied to a hard indentor of conical, pyramidal or spherical geometry for a known period of time (Barnes and Tabor 1966).

Investigation of indentation hardness measurements of polycrystalline ice has been limited, but the work of Barnes and Tabor (1966) has revealed the trends of decreasing hardness with increasing load time and an exponential increase in hardness with decreasing temperature. The applied indentation pressure over ice is hydrostatic, and the magnitude of the hydrostatic stress, occurring near the center of the indentation, is about 60% of the overall hardness value.

Barnes and Tabor (1966) performed hardness tests with ice at temperatures between -15 and 0 °C, and the resulting hardness behavior was explained in terms of transient creep for loading times greater than 10 seconds for ice temperatures lower than -1.2 °C. This investigation revealed a marked drop in hardness between the temperatures of -1.2 ±0.3 °C and 0 °C, indicating that flow occurs not only through the mechanism of creep but also by pressure melting. When both ice and water phases are present, the depression of the melting point dT_m can be related to the hydrostatic pressure dP_H by

$$\frac{dT_m}{dP_H} = -\frac{\Delta V}{\Delta S} = -0.073\,°C/MPa \qquad (7)$$

where ΔV and ΔS are the ice-water changes in volume and entropy.

APPROACH AND OBJECTIVES

This study was approached from an engineering viewpoint, with the intent of applying the results to the physical modeling of moving and stationary structures in ice environments. The ultimate goal of an investigation of this type is to identify and possibly control those parameters that have the largest influence on the friction coefficients between ice and various surfaces and that, consequently, significantly affect the performance of engineering structures in ice environments. As the first step towards this goal, this initial study was designed to investigate the relative influence of various parameters on the kinetic friction coefficients between ice and different surfaces and to determine which of those variables would need future in-depth investigation.

The parameters that were identified as most likely affecting the friction factor are:

1. Normal pressure on the specimens.
2. Relative velocity between ice and the material being investigated.
3. Test configuration (Fig. 1).
4. Ambient temperature.

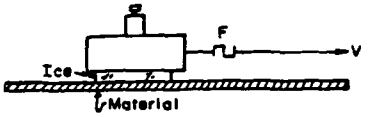

a. Loaded ice sample moving on the sheet of material.

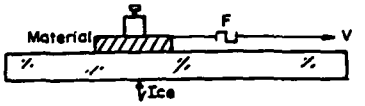

b. Loaded sample of material moving on the ice sheet.

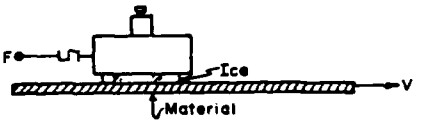

c. Fixed loaded ice sample with the sheet of material moving.

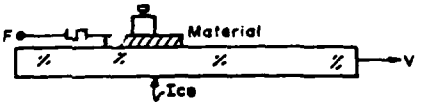

d. Fixed loaded sample of material with the ice sheet moving.

Figure 1. Various friction test configurations of ice moving relative to a material.

Table 1. Summary of friction tests and results from previous investigations.

Test configuration (see Fig. 1)	Materials investigated	Contact surface submerged or wet	Effects of varying *					
			Normal load N or normal pressure P	Sample size s.s.	Velocity v	Material surface roughness R	Thermal conductivity k	Hardness H
Bowden and Hughes (1939) (1d) Sample of material on rotating ice table.	None applicable to this study.	–	No effect with low loads. Heavy loads: $\mu_k\uparrow$ as $P\uparrow$ when $T = 0°C$. $\mu_k\downarrow$ as $P\uparrow$ when $T < -1°C$. $0 < N \leq 300$ g.	None. $0.02 \leq s.s \leq 3.1\ cm^3$, $v = 400$ cm/s.	Certain range had no effect but $\mu_k{}^*$ for low velocities.	–	$\mu_k\uparrow$ as k^*	–
Barnes et al. (1971) (1a) Tip of ice cone sliding over materials.	None applicable to this study.	–	$\mu_k \propto P$ $300 < N < 1175$N $T = -11.75°C$.	–	μ_k vs. v resulted in bell-shaped curve for granite.	–	–	–
Enkvist (1972) Towing (1b) sleds and metal plates over ice. (1a) Ice over test surface.	Aluminum and various steels.	–	(1b) $\mu_k\downarrow$ as $P\uparrow$ $(1.3 < P < 16$ kPa) and μ_k constant when $P > 16$ kPa. $T_0 = -5°C$, $v = 0.6$ m/s.	–	(1b) None when $0.25 \leq v \leq 1.75$ m/s.	(1a) μ_k depended on type of R, not degree of R	–	–
Ryvlin (1973) Towing (1b) steel over freshwater ice; (1a) saltwater ice over steel.	Steel.	(1b) No effect on μ_k.	(1b) $\mu_k\downarrow$ as $P\uparrow$ for $P < 10$ kPa, none when $P > 10$ kPa.	–	(1b) None	(1a) $\mu_k\downarrow$ for R^*	–	–
Evans et al. (1976) (1d) Pendulum-type apparatus. Sliders on rotating drum of ice.	Copper, Perspex and mild steel.	–	–	Affects μ_k but specific relationship not mentioned	$\mu_k\uparrow$ as $s^{-1/2}$ for $0.2 \leq v \leq 10$ m/s $T = -11.5°C$	Affects μ_k but specific relationship not mentioned.	$\mu_k\uparrow$ as $k\uparrow$	Theory $\mu_k\uparrow$ as $H\downarrow$
Saeki et al. (1979) (1a) Sample of cylindrical ice moving over test surfaces.	Concrete plates, various steel plates.	–	None when $100 \leq P < 1000$ kPa, $-3.8 \leq T \leq -2.3°C$, $1.3 \leq v \leq 1.4$ cm/s rough carbon steel.	–	None when $0.07 \leq v \leq 8$ cm/s, $-5°C \leq T \leq -4°C$, $P = 196$ kPa rough carbon steel.	Influences friction factor.	–	–
Vance (1980) (1a) Towing ice block over test surface	Steel: uncoated and coated with Inerta 160.	–	$\mu_k\downarrow$ as $P\uparrow$ $9 \leq P \leq 25$ kPa.	–	$\mu_k\uparrow$ as v^* $v = 6.86$ or 15.8 cm/s.	$\mu_k\uparrow$ as $R\uparrow$.	–	–
Tusima and Tabata (1979, 1981) (1c) Table of test material moving beneath ice sample.	Steel.	No effect on μ_k	None when $2.9 \leq P \leq 226$ kPa, $T = -5°C$, $v = 10^{-4}$ or 2×10^{-3} m/s.	None	$\mu_k\downarrow$ as $v\uparrow$ $3.5\times10^{-7} \leq v \leq 5\times10^{-2}$ m/s, $T = -5°C$.	$\mu_k\uparrow$ as $R\uparrow$.	–	–
Calabrese and Buxton (1980) Calabrese and Murray (1982) (1b) Ring of material rotating on plate of ice.	Ice, steel, concrete and Inerta 160.	–	–	–	$\mu_k\downarrow$ as $v\uparrow$ $1 \leq v \leq 100$ cm/s, $P = 275$ kPa, $T = -18°C$ 1018 steel.	Slight, $\mu_k\uparrow$ as $R\uparrow$. $T = -22°C$, $P = 310$ kPa.	–	–
Oksanen (1980, 1983) (1d) Fixed, loaded slider on a rotating turntable of ice.	–	μ_k for wet ice five times greater than μ_k for dry ice.	$\mu_k\downarrow$ as $P\uparrow$ $0.82 \leq P \leq 4.1$ kPa.	–	$\mu_k \propto v^{-1/2}$ at $-15°C$; $\mu_k \propto v^{1/2}$ at $-1°C$ ice on ice tests.	–	Theory: at low temperature $\mu_k\uparrow$ as $k\uparrow$.	Theory $\mu_k \propto H^{-1/2}$.

*Arrow pointing upward means the variable's value increased; arrow pointing downward means the opposite.

present during these tests may have influenced the dependence of the friction coefficient on various parameters. Oksanen's tests with wet ice resulted in a friction factor five times greater than the friction coefficient for dry ice, but the basic variation in the friction factor with changing parameters was the same for both dry ice and wet ice.

The experimental methods of determining the behavior and magnitude of the friction coefficient between ice and different materials vary greatly, depending on the investigators involved. The results of the studies previously discussed do not always agree; for easy reference a summary of the results of interest to this study is given in Table 1.

the meltwater produced at the ice surface. He made several assumptions when deriving the equation for the coefficient of kinetic friction between ice and a material. He assumed that the frictional force was the result of viscous shear in the meltwater layer between ice and a material, that the velocity distribution in this water layer was linear, that the temperature of the contact surface between the two materials remained at the melting point of ice and that the heat transfer from contact surface into the bulk solids was transient, with a linear temperature distribution in the direction perpendicular to that contact surface. He made no distinction according to whether heat was conducted into the ice or the interacting material. He also assumed that the real contact area A between the sliding surfaces was square with a side x, and that the total area consisted of a number n of small contacts at surface asperities so that $A = nx^2$.

According to Oksanen's theory, the general behavior of the coefficient of friction between ice and material depends on the ambient temperature. At low temperatures the friction factor varies with $v^{-1/4}$ according to the equation:

$$\mu = n^{1/4} H_1^{-1/4} N^{-1/4} \sqrt{1/2v}$$

$$(\Delta T_1 \sqrt{k_1 c_1 \varrho_1} + \Delta T_2 \sqrt{k c_2 \varrho_2}). \qquad (5)$$

On the contrary, when the ambient temperature is close to 0 °C, the friction factor varies with $v^{1/4}$ according to

$$\mu = \sqrt{\frac{\eta_0 v h \varrho_0 x}{N H_1}} = n^{1/4} H_1^{-1/4} N^{-1/4} \sqrt{\eta_0 v h \varrho_0} \qquad (6)$$

where H_1 = N/A, the indentation hardness of ice
$\Delta T_{1,2}$ = temperature difference between the contact surface and the bulk solid (subscript 1 = ice, subscript 2 = material interacting with ice)
c_1 = specific heat capacity of ice
c_2 = specific heat capacity of interacting material
ϱ_0 = density of water
ϱ_1 = density of ice
ϱ_2 = density of interacting material
h = latent heat of melting for ice.

Equation 5 determines the friction coefficient when ΔT_1 is larger than approximately 10 °C. A very thin water layer whose thickness is nearly constant is present at the contact surface. If the amount decreases, more frictional heat results for want of lubrication. The increase in frictional heat causes more surface melting, which replenishes the water layer. An increase in the thickness of the water layer will reduce frictional heating, resulting in a temperature drop at the contact surface below the melting point of the ice. Because of the "self-balanced" nature of the water layer, the majority of the frictional heat is conducted into the two interacting solids, and the friction is thus determined by the conduction of heat. At higher velocities the period for heat conduction is shorter, and the penetration depth more shallow. Consequently, a portion of frictional heat greater than that required for the self-balancing of the water layer remains for melting the ice surface. A thicker water layer is produced, the lubrication effects are greater and the friction factor decreases.

When the ambient temperature is close to 0 °C, according to eq 6, the majority of the heat produced by friction is consumed by melting the surface layer of ice. The thickness of this layer of meltwater is proportional to $v^{1/4}$ and the frictional force is determined by the viscous shear in the water layer.

In order to study the effect of normal load, temperature and velocity on the coefficient of friction, Oksanen performed tests using an apparatus that consisted of a fixed, loaded slider mounted above a turntable of ice.

The coefficient of friction between ice and all tested materials decreased as normal loads increased. However, the variation was not always proportional to $N^{-1/4}$ as predicted by theory. Oksanen justified the deviation from theory by citing an inaccurate estimate of the geometry of the contact area and the increased initial ploughing of the ice with increased load.

Only rough conclusions about the influence of velocity on the friction coefficient could be made based on the results of Oksanen's tests. The theory of eq 5 and 6 was supported by the experiments. However, these trends were not apparent for all the tested materials. Since the theory depends on the water layer largely influencing the friction coefficient, the dependence of the friction factor on velocity may vary if the water layer is disturbed by loose ice powder at the contact surface, for example. Such disturbance may have been the cause for the friction factor to appear independent of velocity.

Oksanen also conducted friction tests with wet ice to determine if the friction coefficient behaved differently than it did for dry ice. The extra water

load to the indentor may vary according to the operator performing the hardness test Consequently, indentation tests of similar ice may differ from one operator to another, and comparisons between results of various investigations would most likely be invalid.

Variation of kinetic friction between ice samples and a sheet of material

Effect of sample size

First, it was important to determine if scale effects significantly influenced the friction factor over the range of sample sizes used during this study. Tests were conducted in the sample room with samples of ice sliding over a stainless steel sheet with an RA value of 0.36 μm. The sliding velocity was approximately 10 cm/s, and a normal pressure of 10 kPa was maintained by varying the normal load. The average value of x_i measured during the ice hardness test was 0.28 mm, corresponding to a hardness value of 1800 kPa according to eq 10. The results of this set of tests with top ice are listed in Table B1 and are presented on Figure 16.

Figure 16 shows that within the range of sample surface areas of 16–400 cm^2 there are no significant scale effects on the kinetic friction factor between top ice and stainless steel. The average coefficient of kinetic friction was 0.041. Tests performed with samples of bottom ice over this same size range also showed no scale effects on μ_k. These results indicate that the surface of each sample size used during this study represented the average ice surface and was not biased by single ice crystals.

Effect of relative motion

In order to determine the effects of relative motion on the kinetic friction coefficient between an ice sample and a stainless steel sheet, the results of tests under configuration a (Fig. 1) were compared with those under configuration c. A sample of ice was towed over a stationary sheet of stainless steel, and then a sample of ice from the same sheet was held stationary while the steel sheet was pulled beneath it. The relative velocity was approximately 5 cm/s, and the samples of both top and bottom ice were subject to a normal pressure of 10 kPa. The frictional force required to tow the sample of configuration a was compared to the frictional force required to hold the sample of configuration c stationary. There was no variation in μ_k with changes in relative motion, indicating that the test method is not biased by these apparatus configurations.

Effects of normal pressure and ice hardness

Sample room tests were conducted to determine the variation of kinetic friction with varying normal pressure. Samples of top ice were pulled over a stainless steel sheet (0.36 μm RA) at a velocity of approximately 10 cm/s. Although these tests were performed with ice of only three different hardnesses (the data are listed in Table B2 and presented on Fig. 17), an effect of ice hardness on ice-stainless steel friction was observed.

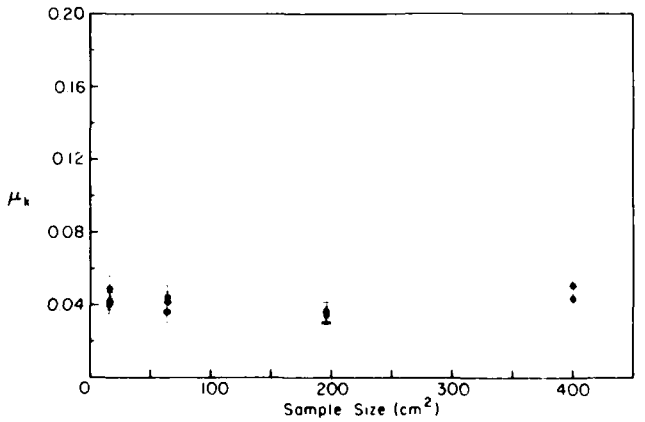

Figure 16. The influence of scale effects on the coefficient of kinetic friction μ_k. Top ice sample sliding over stainless steel sheet (P = 10 kPa, v = 10 cm/s, H$_i$ = 1800 kPa, R = 0.36 μm RA).

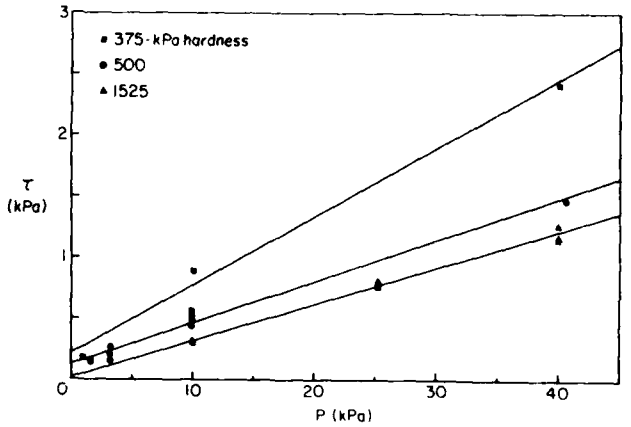

Figure 17. Variation of frictional shear stress τ with normal pressure P. *Ice with three different hardnesses was tested. Samples of top ice were pulled over a stainless steel sheet (0.36 μm RA, v = 10 cm/s).*

Figure 17 shows that the frictional shear stress τ increases linearly with increasing normal pressure P, that is

$$\tau = \alpha P + \tau_0 \qquad (11)$$

where $\tau = F/A_s$, F is the frictional force and A_s is the surface area of the ice sample. Comparison of the results indicates that a decrease in ice hardness leads to an increase in both the slope α and the y-intercept τ_0 of frictional shear stress versus normal pressure. For the hardest ice tested (x_i = 0.33 mm, H_i = 1525 kPa), the calculated values of α and τ_0 are 0.030 and 0.018, respectively. For ice with a hardness index of 500 kPa (x_i = 1.09 mm), the variation of μ_k with increasing normal pressure is characterized by α = 0.034 and τ_0 = 0.125. Finally, for ice with a hardness index of 375 kPa (x_i = 1.49 mm), it was found that α = 0.056 and τ_0 = 0.215. It should be noted that both α and τ_0 initially decrease very quickly with increasing hardness, and that α tends to become constant for H_i > ˙000 kPa while τ_0 is practically zero for H_i > 1400–1500 kPa, as shown on Figure 18.

These data indicate that the kinetic friction between ice and stainless steel follows the behavior described by Rabinowicz (1965), where τ_0 is interpreted as the effect of adhesion between the contact surfaces. The rapid increase of adhesion with decreasing hardness is attributed to the larger area

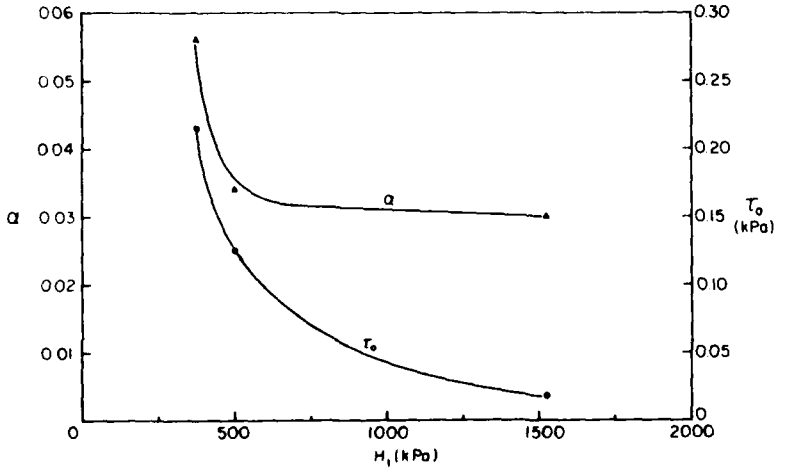

Figure 18. Stress caused by ice adhesion τ_0 and the ratio α of frictional shear stress to normal pressure versus the ice hardness value H_i.

of actual contact between soft ice and steel. Adhesion is also greater for a material with a low elastic modulus (Rabinowicz 1965). It has been observed that a decrease in ice hardness is related to a decrease in flexural strength. This decrease in σ_f is accompanied by a decrease in the elastic modulus, depending on temperature and ice thickness (Timco 1979, Hirayama 1983), which results in an increase in adhesion. The increase of α with decreasing hardness may be explained in a similar manner. As hardness decreases, the area of actual contact between the surfaces increases, resulting in greater interaction of asperities and greater friction.

The corresponding variation of the kinetic friction factor, which was defined as $\mu_k = \tau/P$, with normal pressure P is shown on Figure 19. From eq 11 the expression for μ_k is obtained

$$\mu_k = \tau/P = \alpha + \tau_0/P. \qquad (12)$$

If τ_0 is small with respect to the normal pressure, i.e., for relatively hard ice, the kinetic friction coefficient is practically equal to α. On the other hand, if adhesion is relatively large, for soft ice, τ_0/P can significantly affect the friction factor. Consequently, the influence of adhesion on the kinetic friction factor is significant at low normal pressures (P < 10 kPa) and low hardness, as shown by the data of Figure 19.

It should be noted that during the friction tests of this study, the pressure distribution along the ice sample surface may not have been uniform and the actual normal pressures applied to the samples may have deviated from the calculated normal pressures. The frictional force was measured at the application point of the pulling force, approximately 25 mm above the actual sliding surface. The resulting moment created by the pulling force and frictional resistance may therefore have caused the normal load to be slightly greater at the leading edge of the sample. In addition, as ice hardness decreases, the actual area of contact increases. Since the normal load remains constant, an increase in contact area will decrease the actual normal pressure. The samples of this set of tests were the same size (surface areas of 14 by 14 cm) with the exception of a few used during experiments with ice of 500-kPa hardness. However, there is close agreement between the results of those tests, indicating that the difference between actual and calculated normal pressures is proportional to sample size.

Effect of velocity

As shown in Figure 20, friction tests conducted in the sample room showed an increase in the kinetic friction factor with increasing velocity when the sample of top ice was pulled over a sheet of smooth stainless steel (Fig. 1a). The steel had a surface roughness of 0.36 μm RA, and a normal pressure of 10 kPa was applied to the ice. The experiments were conducted with ice having hardnesses of 975 kPa and 1175 kPa. Figure 20 shows close agreement of the variations of μ_k with increasing velocity for the ice with similar hardnesses, confirming the repeatability of the test. During tests with ice of both hardnesses, the kinetic fric-

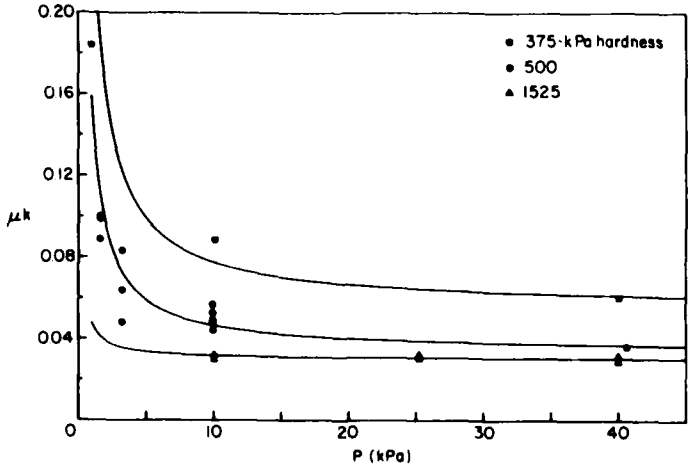

Figure 19. Variation of kinetic friction factor μ_k with normal pressure P *and ice hardness* H_i. *Top ice samples were pulled over a stainless steel sheet (0.36 μm RA, v = 10 cm/s).*

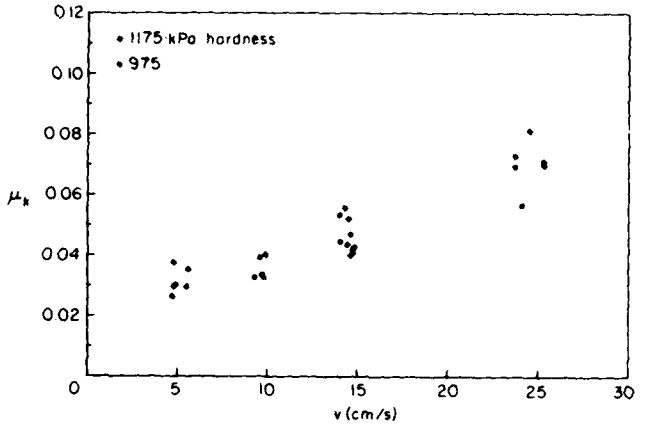

Figure 20. Effect of velocity v on the kinetic friction factor μ_k between a top ice sample and stainless steel sheet (0.36 μm RA, P = 10 kPa).

tion factor increased from 0.03 to 0.07 when the velocity was increased from 5 to 25 cm/s. Table B3 lists the data for this series of tests.

When an ice sample slides over a sheet of steel, the frictional heat is dissipated by conduction into the bulk solids of ice and steel and also by the latent heat of melting. Since the ice sample is a stationary body relative to the heat source, its surface is continually warmed by frictional heating, and a surface layer of meltwater is formed. This water layer will introduce viscous shear stresses, which will add to friction and may become the predominant source of resistance. Oksanen (1980, 1983) showed analytically that for ice friction tests conducted at temperatures close to the ice melting point, as in the present case, most of the additional frictional heat produced at high velocities is dissipated by ice melting. This results in a thicker layer of meltwater, and the kinetic friction coefficient μ_k should then vary as a function of $v^{1/2}$ because of viscous shear of the meltwater layer.

Effects of ice orientation and velocity

Friction tests conducted with samples of ice sliding over a stainless steel sheet (0.36 μm RA) indicated that the orientation of the ice sample has little influence on the kinetic friction coefficient. Figure 21 shows that μ_k for samples of top ice increases from approximately 0.03 to 0.08 as veloci-

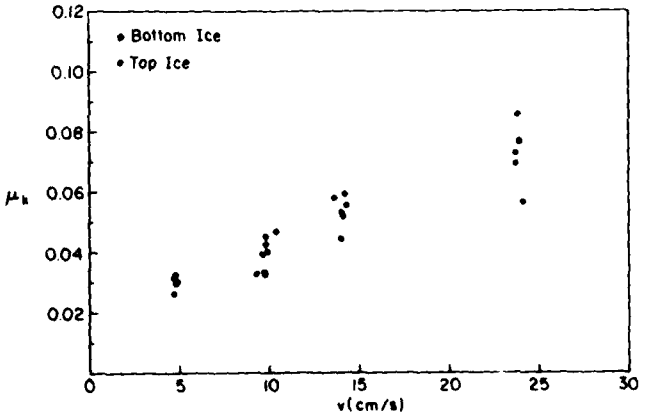

Figure 21. Effect of ice orientation and velocity v on the kinetic friction coefficient μ_k between an ice sample and stainless steel sheet (0.36 μm RA, P = 10 kPa, H_i = 975 kPa).

ty increases from 5 to 25 cm/s, and that of bottom ice from the same sheet increases from 0.03 to 0.06 over the same velocity range. The difference between friction coefficients of top and bottom ice is small, but consistent with the previous results, since the bottom ice is likely to be somewhat softer than top ice because of variation in crystalline structure of the ice across its thickness.

The hardness index of the top ice samples used during this series of tests was calculated as 975 kPa. No hardness measurements were conducted for the bottom ice. A normal pressure of 10 kPa was applied to the ice samples. The data of this set of experiments can be found in Table B4.

Effect of roughness

Top ice samples were pulled over sections of a stainless steel sheet, each section having a different RA value. A sliding speed of approximately 10 cm/s was used, and normal pressures of 10 kPa were applied to the samples. The ice had a hardness index of 1975 kPa. The data for this set of experiments are listed in Table B5.

Figure 22 shows that when the roughness R of the stainless steel sheet was increased slightly from 0.35 to 1.11 μm RA, a large increase in the kinetic friction coefficient resulted. The asperities of the rougher steel surface penetrated the meltwater layer at the contact region. Ice surface deformation during sliding was therefore increased, requiring a greater force to pull the ice sample over the steel. As the stainless steel roughness was increased further from 1.11 to 7.07 μm RA, there was no significant variation in the kinetic friction factor. Since the roughness morphologies varied between the sanded (1.11 μm RA) and the sandblasted surfaces (7.07 μm RA), no definitive explanation can be made for the seemingly constant behavior of μ_k with increasing roughness. However, a possible explanation could be that despite the increase in steel roughness, surface asperities were not able to penetrate the ice surface when the sample slid at 10 cm/s under a normal pressure of 10 kPa. Time and pressure were only sufficient for the asperities to penetrate a certain depth into the ice surface, regardless of the RA value of the steel.

Variation of kinetic friction between samples of material and an ice sheet

Effects of test configuration and velocity

Experiments were conducted in the test basin in order to compare directly the influence of test configurations a and b (Fig. 1) on the variation of μ_k with velocity. Friction measurements were first made for a "smooth" stainless steel sample (0.33 μm RA) sliding over an ice sheet at varying velocities. Following the procedure discussed in the *Test Basin Experiments* section, friction tests of the reverse configuration of towing a top ice sample over the stainless steel sheet (0.36 μm RA) were then immediately performed to ensure that the environmental conditions of the tests were identical, and that the ice was the same for both configurations (H_i = 2800 kPa). A normal pressure of 10 kPa was applied to both the ice and stainless steel samples whose surface areas were 14 by 14 cm. The data for this series of tests are listed in Table B6.

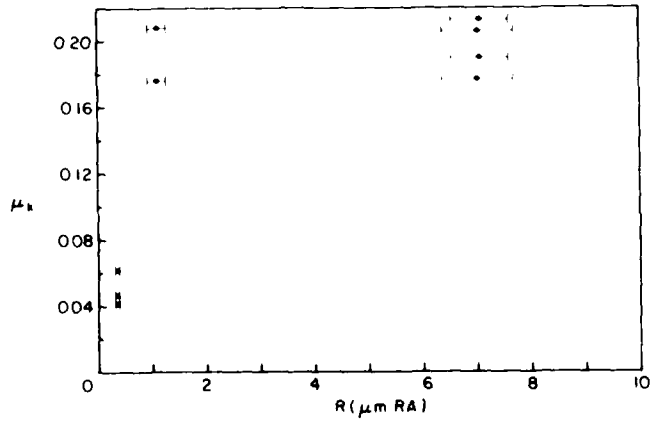

Figure 22. Effect of roughness R on the kinetic friction factor μ_k between samples of top ice and a stainless steel sheet (P = 10 kPa, v = 10 cm/s, H_i = 1975 kPa).

The results of these experiments, shown on Figure 23, reveal a difference in the variation of the kinetic friction factor with increasing velocity depending on the test configuration. The friction factor between a loaded ice sample and the stainless steel sheet increased as velocity increased from 5 to 25 cm/s. Since this behavior was observed as well during the sample room tests as described in the *Effect of Velocity* section, the increase of μ_k with increasing velocity is indeed a characteristic of this test configuration and not an effect of test location, namely sample room versus test basin. On the other hand, the results of tests with a loaded stainless steel sample of the same roughness (0.33 μm RA) sliding over the ice sheet (configuration b of Fig. 1) show no significant variation of the kinetic friction factor with velocity, although there was a slight decrease in friction with increasing velocity.

No fully satisfactory explanation can yet be offered for this difference in the variation of μ_k with velocity between the two test configurations. As mentioned previously, Oksanen (1980, 1983) showed that when the ambient temperature is close to 0°C and the frictional heat is dissipated primarily by melting of the ice, the coefficient μ_k is predicted to vary as a function of $v^{1/2}$. At the other extreme, i.e., for low ambient temperature, when the frictional heat is almost totally dissipated by conduction through the ice and material, Oksanen showed that μ_k ought to vary as a function of $v^{-1/2}$. However, his final formula contained symmetrical terms for the ice and the other test material and, hence, did not differentiate whether it is the ice sample or the material sample that is sliding.

For the type of ice tested in this study, when the loaded ice sample is sliding over an impervious material such as steel, the water layer is replenished not only by frictional melting but also by "brine" drainage from the ice sample. On the other hand, when the steel sample is sliding on top of an ice sheet, there is no upward drainage from the ice; on the contrary, the water layer may be depleted by absorption of water by the underlying ice. In addition, limited time is allowed for an ice asperity to melt when a steel sample slides over it, with the period of time dependent on the velocity of the sample. The short contact period of high velocities is compensated for by the increased frictional melting, and the thickness of the water layer, therefore, remains relatively constant as velocity increases. When a sample of ice slides over the steel sheet, more time is allowed for an ice asperity to melt, and the water layer is likely to be thicker than in the reverse configuration, resulting in a greater contribution of viscous shear to the frictional resistance.

Figure 23 also indicates that at some low velocity the kinetic friction factor between stainless steel and ice is the same for the two test configurations. It is likely that a slow sliding speed will result in similar heat flux and consequent frictional melting for the different testing methods, and that corresponding viscous shear will be relatively small in the case of test configuration a, i.e., ice over steel.

Effects of roughness and velocity

The effect of roughness on the variation of μ_k with velocity is significant for the tests shown on Figure 24. Two stainless steel samples with RA

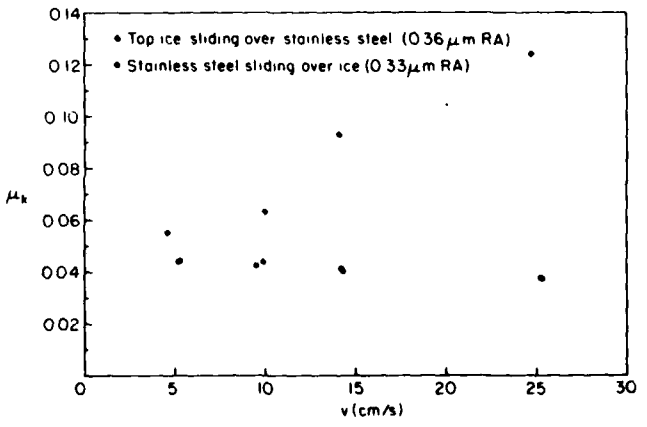

Figure 23. Effect of test configuration and velocity v on the kinetic friction coefficient μ_k (P = 10 kPa, H_i = 2800 kPa, R = 0.3 μm RA).

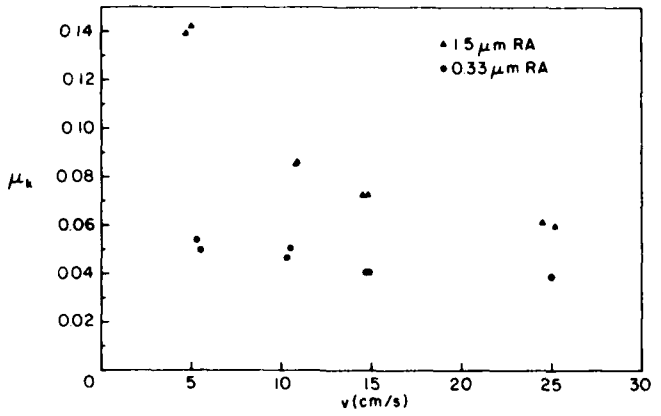

Figure 24. Effect of roughness R *and velocity* v *on the kinetic friction coefficient* μ_k *between stainless steel samples and ice (*P = *10 kPa,* H_i = *2800 kPa).*

values of 0.33 and 1.5 μm were towed over the same ice sheet with hardness index of 2800 kPa. The normal pressure used during these friction tests was 10 kPa. The data are listed in Table B7.

As observed previously, the kinetic friction factor between the smooth stainless steel sample and ice (Fig. 24) did not vary significantly as velocity increased. At most, a slight decrease in μ_k with increasing velocity can be observed, possibly because of greater lubrication at higher velocities. On the other hand, the friction factor of the rougher steel sample (1.5 μm RA), which is consistently larger than that of the smooth sample, shows a marked decrease with increasing velocity.

At 5 cm/s the kinetic friction factor of the rougher steel sample was almost three times greater than that of the smooth sample. This marked increase in the friction factor with increased roughness is likely caused by the Coulomb interaction of the asperities. The meltwater layer is not of sufficient thickness to fill the voids of the rough material surface, and the asperities penetrate the water layer, causing greater deformation of the ice surface and greater friction. As velocity increases a thicker meltwater layer results, filling the voids of the steel surface more completely. Penetration of the water layer is lessened, resulting in a decrease of ice surface deformation. Consequently, the coefficient of kinetic friction between the rough steel sample and ice decreases as velocity increases and appears to tend toward a constant value as shown on Figure 24.

In addition to the possible "cushioning" of the rough steel sample by the meltwater layer at high velocities, as the velocity of the rougher sample is increased from 5 cm/s, the higher sliding speeds will result in less time for the sliding surfaces to interact than is available at lower velocities. Consequently, the surface deformation during sliding is decreased, resulting in a reduced kinetic friction factor.

Effects of roughness and material

Stainless steel and aluminum samples of various roughnesses were pulled over a test basin ice sheet with hardness index of 2800 kPa. The sliding velocity was approximately 10 cm/s, and a normal pressure of 10 kPa was applied to the samples. The data from these tests are listed in Table B8, and a plot of kinetic friction factor versus material roughness is shown in Figure 25.

As the RA values of both materials increase slightly from 0.3 to approximately 1.5 μm, there is a sharp increase in the kinetic friction coefficients. According to the explanation of the *Effect of Roughness* section, when peak heights, or valley depths, of a material surface are introduced to a relatively smooth surface, a marked rise in the friction factor results from the increased surface interaction and ice deformation.

Figure 25 shows that a maximum in the kinetic friction factor occurred for both metals when RA values were approximately 1.5 μm. As surface roughness increased further, there was an apparent decrease in the friction coefficient. It is possible that cohesion or surface tension between the ice and material contact surfaces contributed to the peak values of μ_k, but varying roughness morphologies may also have contributed to this trend. It should be expected that as roughness in-

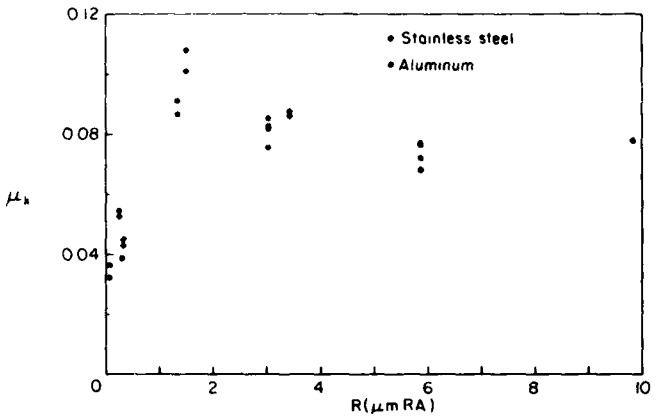

Figure 25. Effect of roughness R *and material on the kinetic friction coefficient* μ_k *between material samples and ice (*P = *10 kPa,* v = *10 cm/s,* H_i = *2800 kPa).*

creases further, μ_k should also start to increase, as the results with the aluminum samples appear to indicate. It would be useful to use higher RA values in future investigations.

Figure 25 also indicates that the kinetic friction coefficients of aluminum are slightly lower than those of stainless steel with similar RA values. However, in most cases the difference is insignificant, and varying roughness morphologies may again contribute to the behavior of the friction factors, causing a slight difference in the values of μ_k for the two metals with similar RA values.

Effects of various materials and velocity

The kinetic friction coefficients between ice with a hardness index of 2800 kPa and samples of stainless steel, aluminum and steel coated with Inerta 160 were compared at different velocities. A normal pressure of 10 kPa was applied to the samples, and RA values of 0.33, 0.30 and 1.6 μm were measured for the samples of stainless steel, aluminum and Inerta 160 respectively. Table B9 lists the data for this set of experiments.

As shown on Figure 26 there is no significant variation of μ_k with increasing velocity for any of the material samples tested. This independence of the kinetic friction factor with varying velocity is expected for samples of smooth material sliding over ice (as discussed in the *Effects of Test Configuration and Velocity* and the *Effects of Roughness and Velocity* sections). The friction factors of the aluminum and stainless steel samples did not

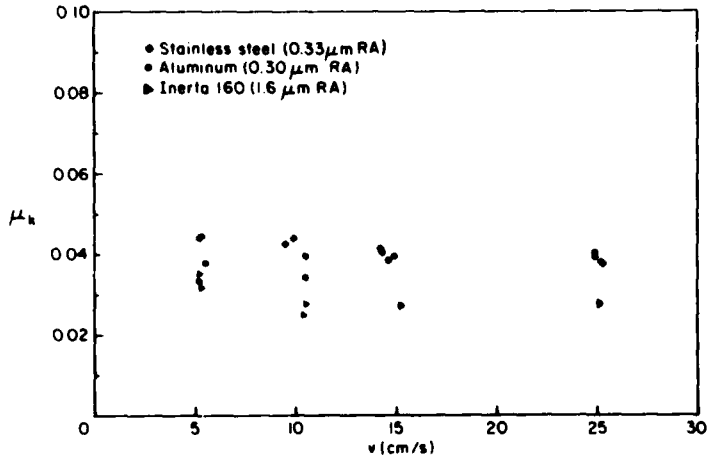

Figure 26. Effect of material and velocity v ***on the kinetic friction factor*** μ_k ***between material samples and ice (*** P = ***10 kPa,*** H_i = ***2800 kPa).***

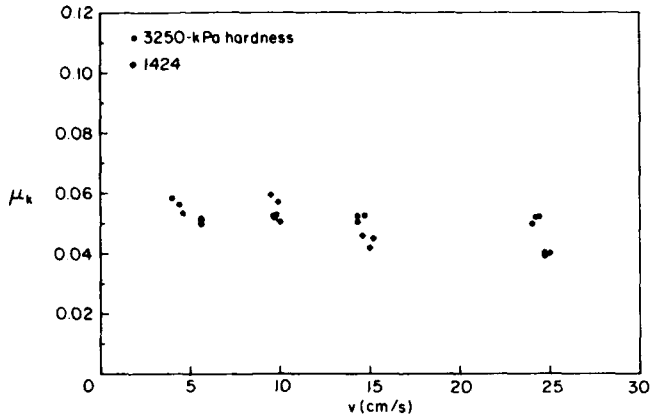

Figure 27. Effect of ice hardness H_i *and velocity* v *on the kinetic friction factor* μ_k *between a sample of stainless steel (0.33 μm RA) and ice (P = 10 kPa).*

vary greatly from one another, but Inerta 160, an abrasion-resistant, low-friction hull coating designed for icebreakers, had the lowest kinetic friction coefficient of approximately 0.03, in spite of its having the largest RA. The Inerta 160 coating has a lower coefficient of thermal conductivity than the metal samples; therefore, less frictional heat is conducted away from the sliding surface into the bulk solid. The additional heat at the contact surface causes increased melting of ice, which in turn may result in greater lubrication and less friction. The low friction coefficient between Inerta 160 and ice may also be attributed to the morphology of the coating surface.

Effects of ice hardness and velocity

Figure 27 shows close agreement of the variations of μ_k with increasing velocity when a smooth stainless steel sample was towed across ice sheets of different hardnesses. The roughness of the steel was 0.33 μm RA, and a normal pressure of 10 kPa was applied to the steel sample. The two ice sheets that were tested had hardness indexes of 3250 and 1425 kPa. Table B10 lists the data of this series of tests.

As discussed in the *Effects of Normal Pressure and Ice Hardness* section, the slope α of the ratio τ/P and the adhesion τ_0 at the contact surface between ice and stainless steel increase as ice hardness decreases (Fig. 17). However, for ice with hardness values H_i greater than 1400–1500 kPa, the value of τ_0 is negligible and α is constant. Consequently, the similar behavior with varying velocity between the friction coefficients of ice with H_i equal to 1425 and 3250 kPa (Fig. 27) can be expected. It can also be noted that test configuration has no apparent effect on the influence of ice hardness on the kinetic friction coefficient between stainless steel and ice with $H_i > 1425$ kPa.

CONCLUSIONS

This investigation of the influence of various parameters on the kinetic friction coefficient between urea-doped columnar ice and various materials, conducted at ambient air temperatures of -1.5 ± 1 °C, yielded the following results:

1. The basic test configuration of the friction experiment (configurations a and c versus b and d of Fig. 1) significantly influences the behavior of the kinetic friction factor with varying relative velocity between ice and smooth stainless steel.

The kinetic friction factor between ice samples and a smooth stainless steel sheet increases as velocity is increased from 5–25 cm/s.

There is no significant influence of velocity over the range 5–25 cm/s on the kinetic friction coefficient between a smooth stainless steel sample and an ice sheet. An increase in velocity may result in a slight decrease in μ_k.

2. The frictional shear stress τ of ice sliding over smooth stainless steel is a linear function of the normal pressure P applied to the ice sample, i.e.,

$$\tau = \alpha P + \tau_0 \qquad (11)$$

where both α and τ_0 were found to be decreasing functions of the ice hardness index H_i. When H_i exceeded a critical value, the adhesion stress τ_0 be-

came practically zero and α became constant. It is judged premature to quantify this critical hardness since it may depend not only on its measurement method but also on the material surface characteristics and type of ice. These results imply that for ice hardness below its critical value, the kinetic friction coefficient, defined as $\mu_k = \tau/P$, is a decreasing function of both P and H_i. For $H_i > (H_i)_{critical}$, μ_k is independent of both P and H_i.

3. A large increase in the kinetic friction factor between ice and materials of stainless steel or aluminum was observed when the roughness average of the material is increased slightly from 0.3 to 1.5 μm. Further increase in roughness up to 10 μm RA had only minor effects on the friction factor.

4. The kinetic friction coefficient between a sample of rough stainless steel (1.5 μm RA) and an ice sheet decreases significantly as velocity is increased from 5 to 25 cm/s, as opposed to the negligible or slightly opposite effect observed with a smooth stainless steel sample (see conclusion 1).

5. The friction coefficients between ice and samples of bare stainless steel and aluminum with nearly identical values of three roughnesses (0.3, 1.3, 3.2 μm RA) did not vary significantly from each other. On the other hand, the friction factor between ice and steel coated with Inerta 160 with an intermediate roughness of 1.6 μm RA was lower than that for the smoothest bare steel and aluminum (0.3 μm RA). These results indicate that the friction coefficient is not only affected by the magnitude of the surface roughness but also by surface and material properties such as roughness morphology and thermal conductivity.

6. For the type of ice used in this investigation, no effect of ice orientation on the friction coefficient between samples of ice and stainless steel was detected.

7. The testing procedure and apparatus used during this investigation yielded repeatable results of the influence of various parameters on the kinetic friction coefficient of ice.

RECOMMENDATIONS

It is obvious that the present study has raised many questions about the physics of ice friction and that further investigations are needed, as suggested below. However, research engineers involved in ice-structure model studies need to characterize the friction factor between ice and the surface of the tested structure. Based on the results of this study, recommendations are proposed for conducting friction tests so that meaningful comparison between different model studies, whether they be in the same laboratory or in different ones, may be made.

Future studies

Based on the experience gained through this study, it is highly recommended that, in any future investigation of the effects of various parameters on the kinetic friction coefficient of ice, tests be conducted in configurations a and b (Fig. 1), loaded ice sample on material and loaded material sample on ice, respectively. In addition, any series of tests designed to investigate the effects of a parameter other than velocity or pressure or both should be repeated for two extreme velocities (e.g., 5 and 25 cm/s) and two extreme pressures (e.g., 5 and 40 kPa), or both. If significant variations in μ_k are noted between the extreme values of either parameter, tests at intermediate values should be made.

Specific parameters that need further investigation are the following:

1. Tests ought to be made over a wider range of roughness, exceeding 10 μm RA.

2. This study, and in particular the parts investigating the effects of velocity and test configuration, should be repeated at lower temperatures where heat dissipation is thought to take place more by conduction than by ice melting.

3. Since some of the trends observed during this study may be ascribable to the properties of urea-doped ice, this investigation should be repeated with ice of radically different structure, such as freshwater ice or snow ice, to eliminate the possible influence of urea concentration and "brine" drainage on the behavior of the kinetic friction coefficient with various parameters.

Friction test procedure in model studies

The following general procedure is proposed for the determination of the kinetic friction coefficient between ice and structure surfaces during model tests of ice-structure interaction. It is based on the limited results obtained so far and is likely to be altered when more studies are compared.

1. The characteristics of the ice and test surface should be as well documented as possible, in particular, type of ice, ice hardness, strength and crystalline structure, type of test surface, surface roughness and surface treatment.

2. The friction test configuration (a or b in Fig. 1) should be selected to duplicate the loading and relative motion of the test. For example, in ice-breaker tests, the ship hull is exerting pressure on

surrounding ice and configuration b may be preferred, while in ice ride-up tests, configuration a may be more appropriate. In case of doubt, both configurations should be used.

3. At least two loading pressures (e.g., 10 kPa and 40 kPa) ought to be used during friction tests to determine whether ice adhesion to the test surface influences the friction factor, especially when the model tests are to be conducted using weak, and thus "soft," ice.

4. Finally, in order to bring to light any variation of the frictional resistance with velocity, friction tests ought to be conducted at a minimum of two extreme velocities or, preferably, over a range of velocities.

The above procedure may appear overly cautious and demanding. However, since the number of model tests in ice for a particular structure are usually kept to a minimum because of their high cost and since frictional forces between ice and test structures are usually significant, it is considered worthwhile to invest sufficient time and effort in friction investigations that are as thorough as feasible.

LITERATURE CITED

Barnes, P. and D. Tabor (1966) Plastic flow and pressure melting in the deformation of ice. I. *Nature,* **210**: 878-882.

Barnes, P., D. Tabor and J.C.F. Walker (1971) The friction and creep of polycrystalline ice. *Proceedings of the Royal Society of London,* **324A**: 127-155.

Bowden, F.P. and T.P. Hughes (1939) The mechanism of sliding on ice and snow. *Proceedings of the Royal Society of London,* **172A**: 280-297.

Calabrese, S.J. and M.G. Buxton (1980) Frictional characteristics of materials sliding against ice. *Lubrication Engineering,* **36**(5): 283-289.

Calabrese, S.J. and S.F. Murray (1982) Methods of evaluating materials for icebreaker hull coatings. In *Selection and Use of Wear Tests for Coatings, ASTM STP 769* (R.G. Bayer, Ed.). Philadelphia: American Society for Testing and Materials, pp. 157-173.

Committee on Ships in Ice-Covered Waters (1981) Report to 16th International Towing Tank Conference. In *Proceedings, 16th ITTC, 31 August to 9 September, Leningrad.* Vol. I, p. 365.

Enkvist, E. (1972) On the ice resistance encountered by ships operating in the continuous mode of ice breaking. The Swedish Academy of Engineering Sciences in Finland, Report No. 24, pp. 54-64.

Evans, D.C.B., J.F. Nye and K.J. Cheeseman (1976) The kinetic friction of ice. *Proceedings of the Royal Society of London,* **347A**: 493-512.

Frankenstein, G. (Ed.) (1975) Report of task committee on standardizing methods for ice. In *Proceedings, Third International Symposium on Ice Properties, 18-21 August, Hanover, New Hampshire,* pp. 607-618.

Hirayama, K. (1983) Properties of urea-doped ice in the CRREL test basin. USA Cold Regions Research and Engineering Laboratory, CRREL Report 83-8.

Michel, B., K. Davar, R. Frederking, R. Gerard, R. Hausser, R. Kry and J. Michel (Ed.) (1981) IAHR recommendations on testing methods of ice. Third report of working group on testing methods in ice. In *Proceedings, IAHR International Symposium on Ice, 27-31 July, Quebec.* Vol. II, pp. 938-952.

Oksanen, P. (1980) Coefficient of friction between ice and some construction materials, plastics and coatings. Espoo: Technical Research Centre of Finland, Laboratory of Structural Engineering, Report 7.

Oksanen, P. (1983) Friction and adhesion of ice. Espoo: Technical Research Centre of Finland, Laboratory of Structural Engineering, Publication 10, pp. 8-16.

Rabinowicz, E. (1965) *Friction and Wear of Materials.* New York: John Wiley and Sons, pp. 3-4, 227-232.

Ryvlin, A.Ya. (1973) Experimental study of the friction of ice. In *Ice Navigation Qualities of Ships* (D. Kheisin and Yu.N. Popov, Ed.). USA Cold Regions Research and Engineering Laboratory, Draft Translation 417, pp. 217-234.

Saeki, H., T. Ono and A. Ozaki (1979) Experimental study on ice forces on a cone-shaped and an inclined pile structure. In *Proceedings, 5th International Conference on Port and Ocean Engineering Under Arctic Conditions (POAC 79), 13-17 August, Trondheim, Norway,* pp. 1081-1095.

Selby, S.M. (Ed.) (1973) *CRC Standard Mathematical Tables.* 21st Ed. The Chemical Rubber Company Press, p. 17.

Schwarz, J. (Ed.) (1979) IAHR recommendations on testing methods of ice properties. Second report from IAHR working group on standardized testing methods in ice. Lulea, Sweden: Division of Water Resources Engineering, University of Lulea, Sweden, Bulletin Series A, No. 24.

Tabata, T. and K. Tusima (1981) Friction measurements of sea ice on some plastics and coatings. In *Proceedings, 6th International Conference on Port and Ocean Engineering Under Arctic Condi-*

tions (POAC '81), Trondheim, Norway. Vol. I, pp. 526–535.

Timco, G.W. (1979) The mechanical and morphological properties of doped ice: A search for a better structurally simulated ice for model test basins. In *Proceedings, 5th International Conference on Port and Ocean Engineering Under Arctic Conditions (POAC '79), 13–17 August, Trondheim, Norway.* Vol. I, pp. 719–739.

Timco, G.W. (1981) On the test methods for model ice. *Cold Regions Science and Technology,* **4**: 269–274.

Tusima, K. and T. Tabata (1979) Friction measurements of sea ice on flat plates of metals, plastics and coatings. In *Proceedings, 5th International Conference on Port and Ocean Engineering Under Arctic Conditions (POAC '79), 13–17 August, Trondheim, Norway.* Vol. I, pp. 741–755.

Vance, G. (1980) Characteristics of ice in Whitefish Bay and St. Marys River during January, February and March 1979. USA Cold Regions Research and Engineering Laboratory, CRREL Special Report 80-32, pp. 6–8.

APPENDIX A: RECOMMENDED FRICTION TESTS

IAHR recommendations

The friction test (Schwarz 1979) should be designed so that the surface of the tested material remains unchanged during the test process. The material surface may be altered, for example, by interaction with sheared ice particles, a smoothing effect due to ice filling the surface cavities, and the wear of surface coatings. Therefore, the material should remain fixed with sliding occurring through the movement of the ice surface. The recommended test configuration for determining the ice friction factor is to tow horizontally a block of ice over dry or wet material surfaces. The sliding surfaces of ice and test material should be a plane, and the leading edge should be free from sharp corners.

Documentation should include descriptions of the ice and material surface as well as measurements of the following parameters:

1. Horizontal towing force free from moments.
2. Total normal force.
3. Dimensions of the ice block.
4. Velocity.
5. Temperature.

Each test should be repeated immediately in the reverse direction to ensure that the inclination of the test surface has no effect on the friction factor. In addition, one data point will represent the average of five to ten of these double measurements.

16th ITTC recommendations

In an effort to ensure consistency in the methods for measuring the coefficient of friction during model tests of an icebreaker, specific experimental conditions were set by the Committee on Ships in Ice-Covered Waters (1981) during the 16th International Towing Tank Conference. The design of the testing technique was left to the individual investigator, but it was mandatory that each include the following requirements established by the committee:

Location:	On standard board provided by National Research Council, Canada (required)
Condition:	Submerged ice and board (required) Surface ice and board (required)
Temperature:	-0.5 °C (required)
Velocity:	10 cm/s
Normal load:	Equivalent to 400 kPa full scale
Ice surface:	Top surface (required) Other surfaces (optional)

APPENDIX B: SELECTED TEST DATA

Table B1. Scale effects attributable to sample size. Loaded top-ice samples (x_i = 0.28 mm) sliding over stainless steel sheet (0.36 μm RA) at -2.2°C. 9 July 1983.

Test No.	μ_k	Sample size (cm x cm)	P (kPa)	v (cm/s)
140	0.049 ± 0.007	4x4	10.0	9.7
141	0.042 ± 0.005	4x4	10.0	9.5
142	0.040 ± 0.005	4x4	10.0	9.6
146	0.044 ± 0.007	8x8	9.9	9.5
147	0.042 ± 0.006	8x8	9.9	9.5
148	0.036 ± 0.006	8x8	9.9	9.5
152	0.036 ± 0.006	14x14	10.0	9.2
153	0.037 ± 0.005	14x14	10.0	9.3
154	0.034 ± 0.005	14x14	10.0	9.3
161	0.050 ± 0.005	20x20	10.0	8.9
162	0.043 ± 0.007	20x20	10.0	9.3

Table B2. Variation of friction factor with normal pressure. Loaded top-ice samples sliding over stainless steel sheet (0.36 μm RA).

Test No.	μ_k	P (kPa)	v (cm/s)
	23 July 1983 x_i = 1.09 mm T_o = -1.7°C		
230	0.100 ± 0.012	1.6	9.5
231	0.099 ± 0.008	1.6	9.3
232	0.089 ± 0.008	1.6	9.3
233	0.057 ± 0.008	9.9	9.3
234	0.053 ± 0.008	9.9	9.3
235	0.048 ± 0.009	9.9	9.3
236	0.083 ± 0.009	3.2	9.2
237	0.064 ± 0.007	3.2	9.3
238	0.048 ± 0.006	3.2	9.4
239	0.036 ± 0.007	40.6	9.3
240	0.049 ± 0.009	9.9	9.3
241	0.049 ± 0.009	9.9	9.4
242	0.044 ± 0.007	9.9	9.4
	30 July 1983 x_i = 0.33 mm T_o = -1.7°C		
299	0.032 ± 0.006	10.0	10.0
300	0.030 ± 0.006	10.0	10.3
301	0.030 ± 0.006	10.0	9.9
302	0.032 ± 0.006	25.2	9.8
303	0.031 ± 0.006	25.2	9.7
304	0.030 ± 0.006	25.2	9.7
308	0.032 ± 0.006	40.0	9.4
309	0.029 ± 0.006	40.0	9.5
310	0.029 ± 0.006	40.0	9.4
	10 September 1983 x_i = 1.50 mm T_o = -2.2°C		
531	0.060 ± 0.004	40.0	8.6
532	0.089 ± 0.008	10.1	9.1
533	0.184 ± 0.027	1.0	9.3

Table B3. Effect of velocity on the kinetic friction factor. Loaded top-ice samples (14 by 14 cm) sliding over stainless steel sheet (0.36 μm RA) at -1.7°C and P=10.0 kPA.

Test No.	μ_k	v (cm/s)
	24 July 1983 x_i = 0.53 mm	
255	0.073 + 0.009	23.7
256	0.057 ± 0.008	24.1
257	0.069 ± 0.009	23.7
258	0.056 ± 0.008	14.3
259	0.053 ± 0.007	14.0
260	0.045 ± 0.006	14.0
261	0.034 ± 0.006	9.7
262	0.040 ± 0.006	9.9
263	0.039 ± 0.006	9.6
264	0.033 ± 0.006	9.3
265	0.030 ± 0.005	4.9
266	0.030 ± 0.006	4.8
267	0.026 ± 0.006	4.7
268	0.033 ± 0.006	9.8
	28 July 1983 x_i = 0.43 mm	
282	0.038 ± 0.007	4.8
283	0.035 ± 0.007	5.6
284	0.030 ± 0.007	5.5
285	0.052 ± 0.006	14.5
286	0.047 ± 0.007	14.6
287	0.044 ± 0.006	14.4
289	0.081 ± 0.010	24.5
290	0.071 ± 0.009	25.3
291	0.070 ± 0.010	25.3
292	0.043 ± 0.006	14.8
293	0.041 ± 0.006	14.7
294	0.040 ± 0.006	14.6
295	0.042 ± 0.006	14.7

Table B4. Variation of the kinetic friction factor with ice orientation and velocity. Loaded ice samples (14 by 14 cm, x_i = 0.53 mm) sliding over stainless steel sheet (0.36 μm RA) at -1.7°C and P=10.0 kPa. 24 July 1983.

Test No.	μ_k	v (cm/s)
	Bottom Ice	
243	0.033 ± 0.005	4.8
244	0.032 ± 0.005	4.7
246	0.043 ± 0.006	9.8
247	0.045 ± 0.006	9.8
248	0.047 ± 0.007	10.4
249	0.052 ± 0.006	14.1
250	0.060 ± 0.006	14.2
251	0.058 ± 0.008	13.6
252	0.077 ± 0.009	23.9
253	0.086 ± 0.008	23.8
254	0.076 ± 0.007	23.9
	Top Ice	
255	0.073 ± 0.009	23.7
256	0.057 ± 0.008	24.1
257	0.069 ± 0.009	23.7
258	0.056 ± 0.008	14.3
259	0.053 ± 0.007	14.0
260	0.045 ± 0.006	14.0
261	0.034 ± 0.006	9.7
262	0.040 ± 0.006	9.9
263	0.039 ± 0.006	9.6
264	0.033 ± 0.006	9.3
265	0.030 ± 0.005	4.9
266	0.030 ± 0.006	4.8
267	0.026 ± 0.006	4.7
268	0.033 ± 0.006	9.8

Table B5. Effect of steel sheet roughness on the kinetic friction factor. Loaded top-ice samples (14 by 14 cm, x_i = 0.25 mm) pulled over stainless steel sheet at -2.2°C and P=10.1 kPa. 9 September 1983.

Test No.	μ_k	R (μm)	v (cm/s)
523	0.213 ± 0.022	7.07	8.7
524	0.190 ± 0.027	7.07	9.1
525	0.208 ± 0.024	1.11	8.8
526	0.176 ± 0.022	1.11	8.9
527	0.062 ± 0.009	0.35	9.5
528	0.047 ± 0.007	0.35	9.5
529	0.206 ± 0.022	7.03	8.8
530A	0.177 ± 0.032	7.03	8.8
530B	0.042 ± 0.005	0.35	9.6

Table B6. Effects of test configuration and velocity on the kinetic friction coefficient. Top ice (x_i = 0.18 mm) moving relative to stainless steel at -2.2°C. Sample size of 14 by 14 cm. 26 August 1983.

Test No.	μ_k	v (cm/s)
	Loaded Steel Sample on Ice R = 0.33 μm P = 9.9 kPa	
424	0.037 ± 0.007	25.3
425	0.038 ± 0.009	25.2
426	0.041 ± 0.006	14.2
427	0.040 ± 0.007	14.3
428	0.044 ± 0.005	5.2
429	0.044 ± 0.005	5.3
430	0.044 ± 0.006	9.9
431	0.043 ± 0.006	9.5
	Loaded Ice Sample on Steel R = 0.36 μm P = 10.2 kPa	
432	0.063 ± 0.009	10.0
434	0.055 ± 0.004	4.6
437	0.093 ± 0.009	14.1
440	0.124 ± 0.012	24.7

Table B7. Variation of the kinetic friction factor with roughness and velocity. Loaded stainless steel samples (14 by 14 cm) sliding over top ice (x_i =0.18 mm) at -1.7°C and P=9.9 kPa. 6 September 1983.

Test No.	μ_k	v (cm/s)
	R = 1.50 μm	
485	0.061 ± 0.012	24.5
486	0.060 ± 0.008	25.2
487	0.073 ± 0.015	14.8
488	0.072 ± 0.008	14.5
489	0.086 ± 0.009	10.9
490	0.085 ± 0.011	10.8
491	0.142 ± 0.013	5.0
492	0.139 ± 0.019	4.7
	R = 0.33 μm	
493	0.054 ± 0.007	5.3
494	0.050 ± 0.006	5.5
495	0.039 ± 0.008	25.0
496	0.039 ± 0.007	25.0
497	0.041 ± 0.011	14.9
498	0.041 ± 0.018	14.7
499	0.051 ± 0.010	10.5
500	0.047 ± 0.007	10.3

Table B8. Effects of roughness and material on the kinetic friction coefficient. Loaded stainless steel and aluminum samples (14 by 14 cm) pulled over top ice (x_i = 0.18 mm) at -2.2°C.

Test No.	μ_k	R (μm)	v (cm/s)
	26 August 1983 Aluminum Samples P = 10.0 kPa		
405	0.077 ± 0.011	5.86	10.4
406	0.068 ± 0.010	5.86	10.1
407	0.072 ± 0.009	5.86	10.2
408	0.082 ± 0.011	3.03	10.3
409	0.076 ± 0.009	3.03	10.1
410	0.032 ± 0.010	0.07	10.0
411	0.036 ± 0.008	0.07	9.8
412	0.039 ± 0.006	0.30	9.7
413	0.039 ± 0.005	0.30	9.8
	26 August 1983 Steel Samples P = 9.9 kPa		
416	0.045 ± 0.006	0.33	9.4
417	0.043 ± 0.005	0.33	9.7
418	0.053 ± 0.012	0.25	9.8
419	0.055 ± 0.009	0.25	9.6
420	0.108 ± 0.009	1.50	9.9
421	0.101 ± 0.009	1.50	9.9
422	0.088 ± 0.009	3.42	10.1
423	0.086 ± 0.010	3.42	10.0
	6 September 1983 Aluminum Samples P = 10.0 kPa		
501	0.078 ± 0.011	9.83	9.9
502	0.078 ± 0.013	9.83	10.2
503	0.076 ± 0.009	5.86	10.0
504	0.068 ± 0.007	5.86	10.1
505	0.085 ± 0.009	3.03	9.8
506	0.083 ± 0.007	3.03	10.0
507	0.091 ± 0.012	1.34	10.1
508	0.087 ± 0.010	1.34	10.1

Table B9. Effects of various materials and velocity on the kinetic friction factor. Loaded material samples (14 by 14 cm) pulled over top ice (x_i = 0.18 mm) at -2.2°C. 26 August 1983.

Test No.	μ_k	v (cm/s)
	Stainless Steel Sample R = 0.33 μm P = 9.9 kPa	
424	0.037 ± 0.007	25.3
425	0.038 ± 0.009	25.2
426	0.041 ± 0.006	14.2
427	0.040 ± 0.007	14.3
428	0.044 ± 0.005	5.2
429	0.044 ± 0.005	5.3
430	0.044 ± 0.006	9.9
431	0.043 ± 0.006	9.5
	Aluminum Sample R = 0.30 μm P = 10.0 kPa	
443	0.040 ± 0.005	24.9
444	0.039 ± 0.006	24.9
445	0.039 ± 0.005	14.9
446	0.038 ± 0.005	14.6
447	0.040 ± 0.005	10.5
448	0.034 ± 0.005	10.5
449	0.038 ± 0.005	5.5
450	0.033 ± 0.004	5.2
	Inerta 160 Samples R = 1.6 μm P = 10.1 kPa	
451	0.035 ± 0.006	5.2
452	0.032 ± 0.006	5.3
453	0.028 ± 0.006	10.5
454	0.025 ± 0.006	10.4
455	0.027 ± 0.006	15.2
456	0.027 ± 0.008	15.2
457	0.028 ± 0.005	25.1
458	0.027 ± 0.005	25.1

Table B10. Variation of kinetic friction factor with ice hardness and velocity. Stainless steel sample (14 by 14 cm, R = 0.33 μm) pulled over top ice with P = 9.9 kPa.

Test No.	μ_k	v (cm/s)
	21 August 1983 x_l = 0.15 mm T_o = -2.2°C	
339	0.053 ± 0.011	9.8
340	0.052 ± 0.009	9.7
341	0.053 ± 0.008	9.6
342	0.053 ± 0.009	4.6
343	0.058 ± 0.011	4.0
344	0.056 ± 0.008	4.4
345	0.053 ± 0.007	14.3
346	0.053 ± 0.009	14.7
347	0.050 ± 0.009	14.3
348	0.052 ± 0.010	24.4
349	0.052 ± 0.006	24.2
350	0.050 ± 0.009	24.0
	23 August 1983 x_l = 0.36 mm T_o = -1.7°C	
376	0.060 ± 0.010	9.5
377	0.057 ± 0.008	9.9
378	0.051 ± 0.008	10.0
379	0.052 ± 0.007	5.6
380	0.051 ± 0.007	5.6
381	0.050 ± 0.006	5.6
382	0.040 ± 0.006	24.7
383	0.040 ± 0.007	25.0
384	0.039 ± 0.007	24.7
385	0.045 ± 0.007	15.2
386	0.046 ± 0.008	14.6
387	0.042 ± 0.008	15.0

APPENDIX C: HARDNESS AND TEMPERATURE HISTORY OF ICE DURING WARMUP

Questions were raised during technical review about the validity of the assumption that the ambient air temperature (-1.5 ± 1 °C) and ice temperature were close to the same during testing. A study was, therefore, undertaken to show that the ice and air temperatures were both likely to be within the specified range, -2.5 ° to -0.5 °C, during the friction tests. Although the CRREL test basin was committed to another investigation at the time of this study, the ice growth conditions and ambient temperature were sufficiently close to those during the friction tests for the results of this investigation to be representative of the conditions of the actual friction tests.

The ice was grown at -12 °C (10 °F) to a thickness of 4.5 cm when the ambient temperature was raised to 1 °C (34 °F). Ice was cut from the test basin sheet and floated in tubs of urea water to simulate the ice used in the sample room friction tests. Calibrated thermistors were used to measure the temperatures of the top surface of the ice in the tub and test basin as well as the ambient air temperature. The hardness of the test basin ice was also determined every time the temperature was measured. The data of this study are listed in Table C1.

Figure C1 shows that within 1 hour after the start of warmup, the temperatures of the ice in

Table C1. Hardness and temperature history of ice during warmup.

Time	Temperature (°C)			Test basin ice hardness
(min)	Ambient air	Tub ice	Test basin ice	(kPa)
50	-5.94	-2.5	-2.4	1650
110	-3.7	-1.9	-1.9	4850
220	-1.8	-1.4	-1.4	2450
345	-0.63	-1.2	-1.1	1800
470	0.3	-0.9	-0.9	1650
590	0.8	-0.8	-0.8	1250
790	0.73	-0.8	-0.8	1975
1520	1.2	-0.6	-0.6	1125

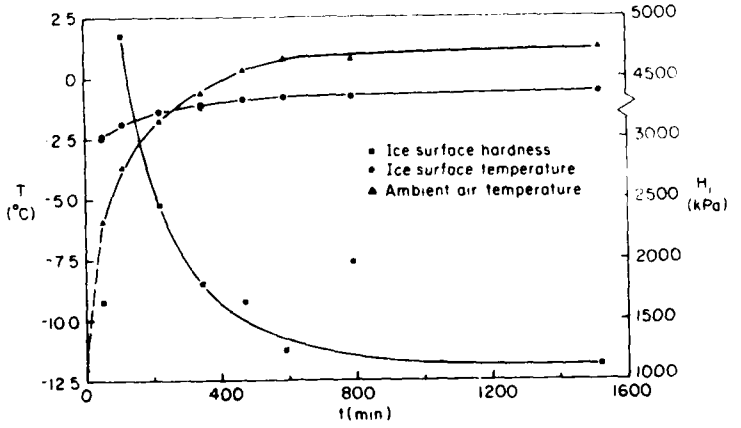

Figure C1. Hardness H, *and temperature* T *history of ice during warmup.*

both the tub and test basin were within the limits of the specified temperature. With the passage of time, the temperatures of the tub and test basin ice never differed significantly from each other and always remained within the range of -2.5° to -0.5°C. In the actual friction experiments, 5 or more hours were allowed to elapse after the ambient air temperature had stabilized at -1.5 ±1°C and before the first friction test was performed. Therefore, the results of this temperature study indicate that the time allowed for the ice to reach thermal equilibrium was more than adequate during the friction coefficient investigation.

Figure C1 also shows that ice hardness decreases only after the passage of considerable time when the ambient temperature has risen above freezing. Because of the on-going unrelated investigation in the test basin, it was not possible to conduct tests on the ice flexural strength; however, it is known that the flexural strength of ice decreases with warmup time and the corresponding increase in temperature (Hirayama 1983). Therefore, this study also confirms, if indirectly, the relationship between the flexural strength and hardness of ice: hardness decreases as flexural strength decreases.

A facsimile catalog card in Library of Congress MARC format is reproduced below.

Forland, Kathryn A.
Kinetic friction coefficient of ice / by Kathryn A. Forland and Jean-Claude P. Tatinclaux. Hanover, N.H.: Cold Regions Research and Engineering Laboratory; Springfield, Va.: available from National Technical Information Service, 1985.
vi, 45 p., illus., 28 cm. (CRREL Report 85-6.)
Bibliography: p. 28.
1. Friction. 2. Ice. 3. Ice engineering. 4. Kinetic friction coefficient. 5. Model tests. I. United States. Army. Cold Regions Research and Engineering Laboratory, Hanover, N.H. III. Series: CRREL Report 85-6.

☆ U. S. GOVERNMENT PRINTING OFFICE: 1985--500-046--22,002


DATE
ILME